

DA030766

Fl.

SDAC-TR-76-6

12

ANALYSIS AND REDUCTION OF FALSE ALARMS AT LASA

A.C. CHANG, R.M. SEGELKE, and R.R. BAUMSTARK

Seismic Data Analysis Center ✓

Teledyne Geotech, 314 Montgomery Street, Alexandria, Virginia 22314

13 MAY 1976

APPROVED FOR PUBLIC RELEASE; DISTRIBUTION UNLIMITED.

Sponsored By

The Defense Advanced Research Projects Agency

Nuclear Monitoring Research Office

1400 Wilson Boulevard, Arlington, Virginia 22209

ARPA Order No. 1920

Monitored By

VELA Seismological Center

312 Montgomery Street, Alexandria, Virginia 22314

DDC
RECEIVED
OCT 30 1976
J.R.

Disclaimer: Neither the Defense Advanced Research Projects Agency nor the Air Force Technical Applications Center will be responsible for information contained herein which has been supplied by other organizations or contractors, and this document is subject to later revision as may be necessary. The views and conclusions presented are those of the authors and should not be interpreted as necessarily representing the official policies, either expressed or implied, of the Defense Advanced Research Projects Agency, the Air Force Technical Applications Center, or the US Government.

Unclassified

SECURITY CLASSIFICATION OF THIS PAGE (When Data Entered)

REPORT DOCUMENTATION PAGE		READ INSTRUCTIONS BEFORE COMPLETING FORM
1. REPORT NUMBER SDAC-TR-76-6	2. GOVT ACCESSION NO.	3. RECIPIENT'S CATALOG NUMBER
4. TITLE (and Subtitle) ANALYSIS AND REDUCTION OF FALSE ALARMS AT LASA	5. TYPE OF REPORT & PERIOD COVERED Technical rept.	
7. AUTHOR(s) Chang, A. C., Seggelke, R. M. and Baumstark, R. R.	8. CONTRACT OR GRANT NUMBER(s) F08606-76-C-0004	
9. PERFORMING ORGANIZATION NAME AND ADDRESS Teledyne Geotech 314 Montgomery Street Alexandria, Virginia 22314	10. PROGRAM ELEMENT, PROJECT, TASK AREA & WORK UNIT VT/6709	
11. CONTROLLING OFFICE NAME AND ADDRESS Defense Advanced Research Projects Agency Nuclear Monitoring Research Office 1400 Wilson Blvd.-Arlington, Virginia 22209	12. REPORT DATE 13 May 1976	13. NUMBER OF PAGES 50
14. MONITORING AGENCY NAME & ADDRESS (if different from Controlling Office) VELA Seismological Center 312 Montgomery Street Alexandria, Virginia 22314	15. SECURITY CLASS. (of this report) Unclassified	
15a. DECLASSIFICATION/DOWNGRADING SCHEDULE		

DISTRIBUTION STATEMENT (of this Report)

~~APPROVED FOR PUBLIC RELEASE; DISTRIBUTION UNLIMITED.~~

H.C. / Chang, R.M. / Seggelke

17. DISTRIBUTION STATEMENT (of the abstract entered in Block 20, if different from Report)

R.K. / Baumstark

18. SUPPLEMENTARY NOTES

F08606-76-C-0004
✓ ARPH / Order - 2551

19. KEY WORDS (Continue on reverse side if necessary and identify by block number)

LASA
False Alarms
LASA False Alarms
Event Processor

20. ABSTRACT (Continue on reverse side if necessary and identify by block number)

We show that many of the "false alarms" which require analyst intervention in the preparation of the LASA event summary were due to local or regional events. Analyses showed that these false alarms occur predominantly on weekdays during local working hours, suggesting that the seismic events are of man-made origin. The false alarm rate decreases on weekends and holidays, and LASA reports more teleseismic events.

408258

y/B

Unclassified

SECURITY CLASSIFICATION OF THIS PAGE(When Data Entered)

To reduce the number of false alarms it is necessary to steer detection beams to local areas. By detecting local events on these beams and by using a higher S/N threshold in processing these signals, we can effectively reduce the number of false alarms from the original 57% to 41%.

A new beam set has been developed and deployed which concentrates tele-seismic beams in high seismicity areas instead of spacing them equidistantly apart. This arrangement reduced the average detection errors from 200 km to 50 km, there is also some indication of a lowered detection threshold on the order of 0.1 ± 0.1 magnitude units.

Unclassified

SECURITY CLASSIFICATION OF THIS PAGE(When Data Entered)

ACCESSION for	
RTIS	White Section <input checked="" type="checkbox"/>
DDC	Buff Section <input type="checkbox"/>
UNANNOUNCED	<input type="checkbox"/>
JUSTIFICATION	
BY	
MULTIPLICATION/STAMP FILE CODES	
A	

ANALYSIS AND REDUCTION OF FALSE ALARMS AT LASA

SEISMIC DATA ANALYSIS CENTER REPORT NO.: SDAC-TR-76-6

AFTAC Project Authorization No.: VELA T/67C9/B/ETR

Project Title: Seismic Data Analysis Center

ARPA Order No.: 2551

ARPA Program Code No.: 6F10

Name of Contractor: TELEDYNE GEOTECH

Contract No.: F08606-76-C-0004

Date of Contract: 01 July 1975

Amount of Contract: \$2,319,926

Contract Expiration Date: 30 June 1976

Project Manager: Royal A. Hartenberger
(703) 836-3882

P. O. Box 334, Alexandria, Virginia 22314

APPROVED FOR PUBLIC RELEASE; DISTRIBUTION UNLIMITED.

DDC
 RECORDED
 OCT 14 1976
 RECEIVED
 D

ABSTRACT

We show that many of the "false alarms" which require analyst intervention in the preparation of the LASA event summary were due to local or regional events. Analyses showed that these false alarms occur predominantly on weekdays during local working hours, suggesting that the seismic events are of man-made origin. The false alarm rate decreases on weekends and holidays, and LASA reports more teleseismic events.

To reduce the number of false alarms it is necessary to steer detection beams to local areas. By detecting local events on these beams and by using a higher S/N threshold in processing these signals, we can effectively reduce the number of false alarms ^{can be effectively reduced} from the original 57% to 41%.

A new beam set has been developed and deployed which concentrates teleseismic beams in high seismicity areas instead of spacing them equidistantly apart. This arrangement reduced the average detection errors from 200 km to 50 km, there is also some indication of a lowered detection threshold on the order of 0.1 ± 0.1 magnitude units.

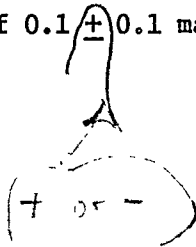


TABLE OF CONTENTS

	Page
ABSTRACT	3
INTRODUCTION	7
CAUSE OF FALSE ALARMS IN THE EVENT PROCESSING SYSTEM	10
DISCUSSION	19
EVALUATION OF THE NEW BEAM SET	21
CONCLUSIONS	30
ACKNOWLEDGEMENTS	31
REFERENCES	32
APPENDIX A - List of Parameters for LBS160	33

LIST OF FIGURES

Figure No.	Title	Page
1	Percentage distribution of EP signals in increments of S/N ratio for the period 24 June to 30 July 1974, when LBS133 was operative.	14
2a	Diurnal distribution of confirmed signals for LBS133.	15
2b	Diurnal distribution of EP false alarm for LBS133.	15
3a	Number of duplicate detections (open circles) and regional-local events (closed circles) at LASA during daytime (0800-1600 local time) from 24 June to 30 July 1974.	18
3b	Number of identified events (squares) and identified later phases (triangles) at LASA during daytime (0800-1600 local time) from 24 June to 30 July 1974.	18
4	World map showing locations of LBS160 beams.	22
5	Comparison of recurrence curves computed for LBS133 and LBS160.	26
6	Percentage distribution of EP signals in increments of S/N ratios for the period from 13 June to 30 June 1975 when LBS160 was operational.	28
7	Comparison of travel time errors for LBS133 beams and LBS160 beams.	29

LIST OF TABLES

Table No.	Title	Page
I	Classification of EP Events from 24 June to 30 July 1974 (Beam Set LBS133).	13
II	Classification of EP Events from June 13 to June 30, 1975 (Beam Set LBS160).	23
III	Classification of EP Events from June 13 to June 30, 1975 with 10 km/sec Velocity Restriction.	24

INTRODUCTION

The on-line data processing of LASA short-period data at the Seismic Data Analysis Center (SDAC) was operational from January 1971 to June 1975. During this period of operation, the main purpose was to produce promptly and routinely an SDAC/LASA daily event summary. The operation of SDAC was temporarily suspended in July 1975 in order to adjust to the instrument and data reconfigurations at LASA, and to implement modifications which would enable SDAC to accept and process seismic data from additional stations.

Data processing is performed in two parts by utilizing two computers. The first part is the Detection Processor (DP) which performs on-line signal detection by forming and applying detection algorithms to a number of surveillance beams. The second part is the Event Processor (EP) which selectively processes detected signals and extracts event parameters such as event location, origin time and magnitude.

The term "false alarm" has been historically used to depict noise detection. False alarm in this sense means detections on fluctuations of noise, and can include instrumental noise such as transmission errors. Efforts to reduce this type of false alarm have been made in the past. Lacoss (1972) argued that since false alarms are detections of noise fluctuations, both noise level and noise variance can affect the rate of false alarms. Studies of noise variance and its effect on signal detectability have been performed at NORSAR (Bungum and Husebye, 1974; Bungum and Ringdal, 1974; and Steinert, Husebye and Gjoystdal, 1975). In particular, Steinert showed that the noise

Lacoss, R. T., 1972, Variation of false alarm rates at NORSAR: Semiannual Technical Summary, June 1972, Seismic Discrimination MIT Lincoln Laboratory, Cambridge, Massachusetts.

Bungum, H. and E. S. Husebye, 1974, Analysis of the operational capabilities for detection and location of seismic events at NORSAR: Bull. Seism. Soc. Am., v. 64, p. 637-656.

Bungum, H. and F. Ringdal, 1974, Diurnal variation of seismic noise and its effect on detectability: NORSAR Scientific Report No. 5-73/74, NTNF/NORSAR, Kjeller, Norway.

Steinert, O., E. S. Husebye, and H. Gjoystdal, 1975, Noise variance fluctuations and earthquake detectability: Geophys. J. R. Astr. Soc., v. 41, p. 289-302.

stability, which is the measure of the ratio of noise average to noise variance, is indeed the most effective indicator of the false alarms. The NORSAR DP is currently operating with varying detection thresholds based on the noise level and noise stability. Chang (1974) argued that if the noise fluctuations can be considered as random occurrences, then the requirement for a number of consecutive threshold crossings would effectively reduce such false alarm detections. In comparing LASA and NORSAR detection algorithms, Chang found that the temporal requirement of consecutive threshold crossings was set to one at NORSAR, but LASA DP required three consecutive crossings. In any case, study of past operations at LASA confirms that noise detections were indeed rare at LASA and did not pose a significant problem to the DP and EP operations.

Chang's comparison of LASA and NORSAR short period array performances shows that in both arrays about 12% of the DP detections are ultimately published as events in daily event summaries. This of course does not mean all DP detections are processed by EP. Of all DP detections approximately one third were processed by EP. An initial reduction of DP detections is made in EP by a higher threshold setting and by a grouping algorithm. Our attention is drawn to the fact that of all signals completely processed by EP, only half of them were confirmed by an analyst and published in the daily summary. In the early evaluation of the LASA/SAAC system, Dean (1972) reported that only 37.3% of EP processed signals were reported on the LASA Daily Summary. If half of the signals processed by EP are false (EP false alarms), the nature of these signals should be investigated. Since it seems clear that DP detections are relatively free of noise detections, we conclude that EP false alarms are seismic signals that cause difficulty in the processing and production of the event bulletin.

In the future SDAC Network Event Processor, carefully selected signals of one station will be associated with detections of other stations. The

Chang, A. C., 1974, A comparison of the LASA-NORSAR short-period arrays: SDAC-TR-74-5, Teledyne Geotech, Alexandria, Virginia.

Dean, W. C., 1972, A geophysical evaluation of the short-period LASA/SAAC system: SAAC Technical Report No. 5, Teledyne Geotech, Alexandria, Virginia.

carefully selected signals are those detections processed with some type of process which will be in fact identical to the EP process. Therefore if these signals contain many false alarms, it will be difficult to obtain good results. In this study false alarms are classified into several categories and analyzed to show the rate of occurrence of each type. Discussions of how false alarms cause detections and possible methods to reduce them are tested with the on-line detection processor.

CAUSE OF FALSE ALARMS IN THE EVENT PROCESSING SYSTEM

The detection threshold of the LASA DP processor has been set to 10 dB. With this threshold, there are approximately 300 detections per day. Not all of these detections are processed by EP. A reduction in the number of detections in EP depends mainly on two conditions: thresholding and grouping. The first condition simply raises the processing threshold to 14 dB, thus eliminating approximately two thirds of the detections. The remaining 100 detections are then screened by the grouping algorithm. The grouping algorithm checks each detection and searches for consecutive detections that are restricted in area and in a specified time window. Only the first detection in the grouped detections is processed. This algorithm further reduces by 30% the number of detections reaching EP. The detections screened through these two conditions are processed by EP on a routine daily basis. There are approximately 70 of such events per day that reach EP for final processing.

The task of the analysts is to examine results of the automatically processed EP events by displaying waveforms and seismic parameters on the Experimental Operations Console (EOC). The analyst can confirm, adjust, submit for reprocessing, or reject the processed event. The final results are published in the SUMMARY OF SDAC/LASA VELOCITY-BEAM LOCATIONS, which contains an average of 30 events per day. The analyst therefore rejects more than 50% of the events that reach EP in daily operations. These rejected events, the EP false alarms, are the main interest of the current analysis.

A data period of 37 days from 24 June to 30 July, 1974, was selected and all EP processed events were studied and grouped into seven categories. These seven categories are: (1) identified events, (2) identified secondary phases, (3) duplicate detections, (4) regional or local events, (5) velocity failures, (6) weak signals, and (7) data dropouts. Categories (1) and (2) contain confirmed signals and the rest are EP false alarms. Definitions of these seven categories are given in the following:

- (1) Identified events: The event has been examined by the analyst and confirmed as a P phase of an event. Events in this category are published in the beam location summary.
- (2) Identified phases: The signal has been confirmed as an arrival of a secondary phase of an identified event. Since the SDAC bulletin does not report events without first confirming P phase, the signals in this category are always associated with category (1).
- (3) Duplicate detections: The signal is apparently detected by a neighboring beam (side lobe detections), or the signal is a coda detection. When waveforms of a duplicate detection are displayed, they are easily recognized and rejected by poor signal alignment throughout subarrays or they are obviously part of the coda of an event.
- (4) Regional or local events: When the signal characteristics vary distinctly from subarray to subarray, it indicates that the signal is a regional or local seismic event arriving at LASA. The variation in signal characteristics is mainly due to the heterogeneity of the crustal structures beneath the array, so that signal coherencies are very poor. In such cases the signal alignment, and the subsequent attempt to define the beam parameters either by machine correlation or analyst adjusted alignments are not reliable. As a result, the analyst rejects the event.
- (5) Velocity failures: The apparent velocity of the signal is higher than the theoretical limit of P phase velocity. The signal could well be a good signal transmitted through the Earth's interior core from a distant location. However, since EP is not presently designed to recognize core phases unless it is being controlled by an analyst, this type of signal is rejected in automatic processing. Note that although this signal is rejected because of operational restrictions, it can be very useful in association with P phase detections from other seismic stations.
- (6) Weak signals: The signal is so weak in amplitude or coherency that neither the computer nor the analyst can find an adequate solution to define a beam. However, it is possible for an experienced analyst to recognize the difference between a weak signal and a signal from a local event.

(7) Data dropouts: The detection is caused by bad samples in the data stream (glitches) or the detection is triggered on a sudden data dropout-restart situation.

The result of analyzing all EP signals during this test period is summarized in Table I. Identified P phases constitute 33.4% of the totals which is comparable to the result of an earlier study made by Dean (1972). The 9.3% in Category 2 is the result of the analyst's effort to identify later phases after the P phase is confirmed. The sum of these two categories, 42.7%, are signals from confirmed events. The remaining 57.3% are EP false alarms of which 36.4% are due to duplicate detections and 11.6% are regional-local events. There are no false alarms due to noise detections, but data dropouts occurred 22 times which amounts to an insignificant 0.8% of the total.

It is clear from Table I that duplicate detections and regional-local events are the dominant causes of EP false alarms. We ask whether we can reduce them by simply raising EP thresholds. In Figure 1 we present again the seven categories of EP signals incrementally grouped in signal-to-noise ratios ranging from 14 to 38 dB. Percentages of each signal category in dB increments are computed and they are shown in a form of histogram. This regrouping shows that the percentage of confirmed events steadily increases as the threshold is raised. However, in order to obtain better than 50% chance of confirmed events, the threshold must be raised to about 24 dB.

The analysis of Figure 1 shows that the distribution of regional-local events is fairly constant throughout all S/N ranges, indicating that close range events are frequently detected whether or not there is a beam directed toward them. The rate of occurrence in each S/N range is approximately 10%. This demonstration clearly indicates that raising the EP threshold will not reduce the false alarms due to regional-local events.

Our analysis shows that there are pronounced diurnal variations of false alarm rates. To demonstrate and investigate diurnal variations of EP false alarms, we regrouped all signals according to local time of the day at LASA. In Figure 2, cumulative hourly frequencies of each signal category are tabulated in terms of local time and presented in two histograms. This analysis

TABLE I

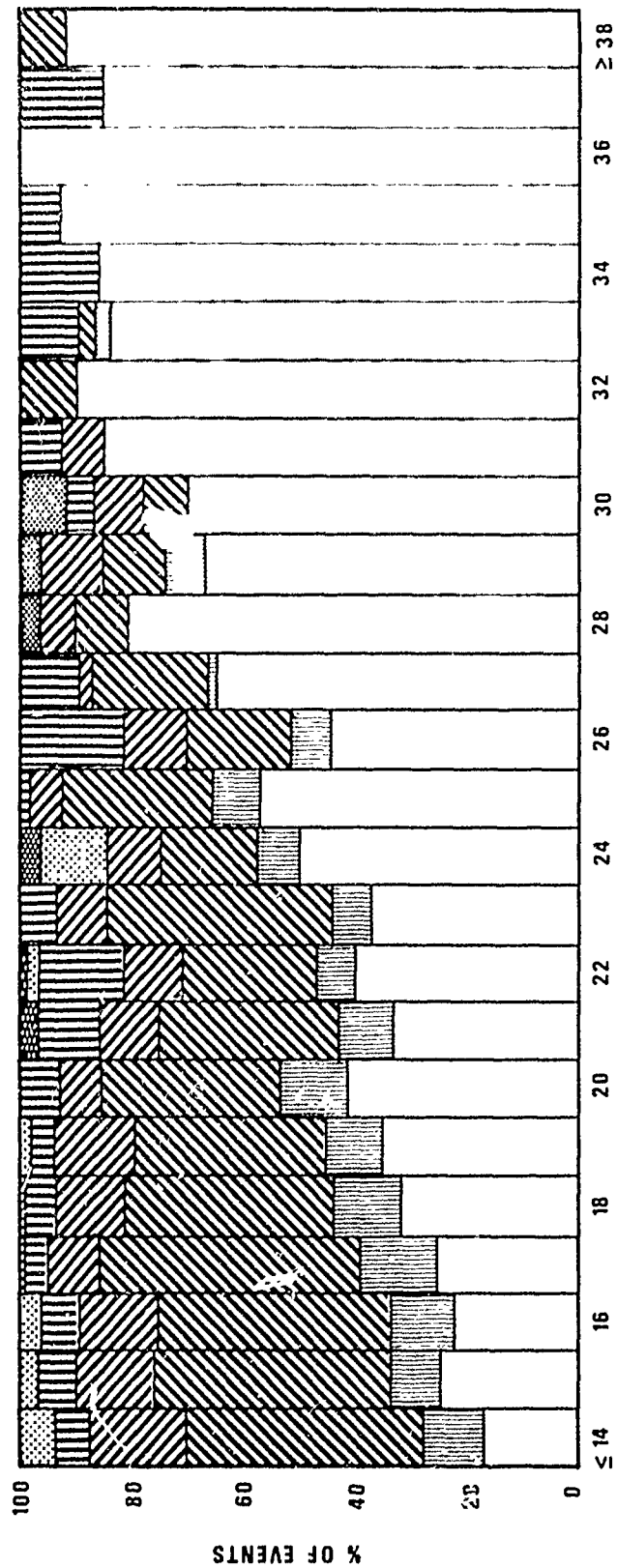
Classification of EP Events from 24 June to 30 July 1974
(Beam Set LBS*133)

Category	Number of Events	%
(1) Identified events	958	33.4
(2) Identified secondary phases	268	9.3
(3) Duplicate detections	1043	36.4
(4) Regional or local events	332	11.6
(5) Velocity failures	176	6.1
(6) Weak signals	69	2.4
(7) Data dropouts	<u>22</u>	<u>0.8</u>
Total	2868	100.0

*LBS = LASA Beam Set

LEGEND

- EDITED AND PUBLISHED
- ▨ DUPLICATE DETECTIONS
- ▧ REGIONAL DETECTIONS
- ▩ VELOCITY FAILURE
- ▤ IDENTIFIED PHASE
- ▥ WEAK EVENTS
- ▦ DATA DROPOUTS



SIGNAL TO NOISE RATIO (db)

Figure 1. Percentage distribution of EP signals in increments of S/N ratio for the period 24 June to 30 July 1974, when LBS133 was operative.

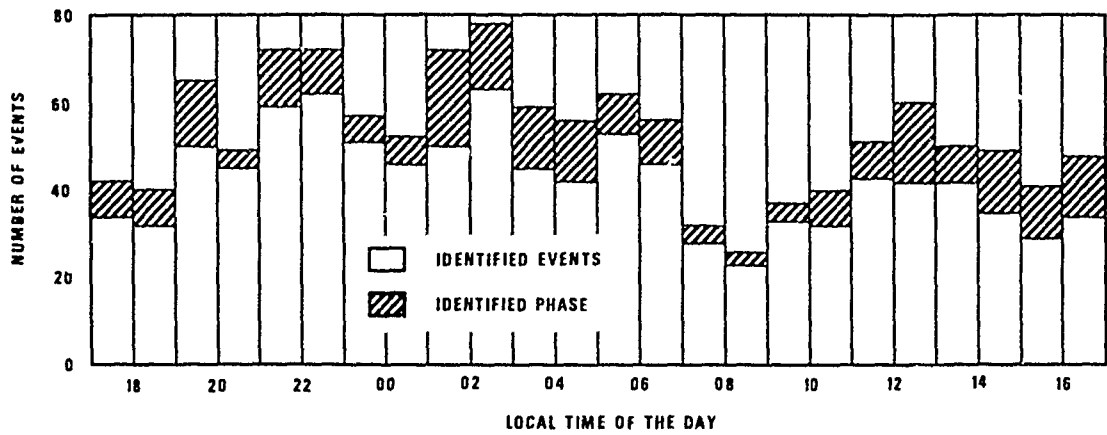


Figure 2a. Diurnal distribution of confirmed signals for LBS133.

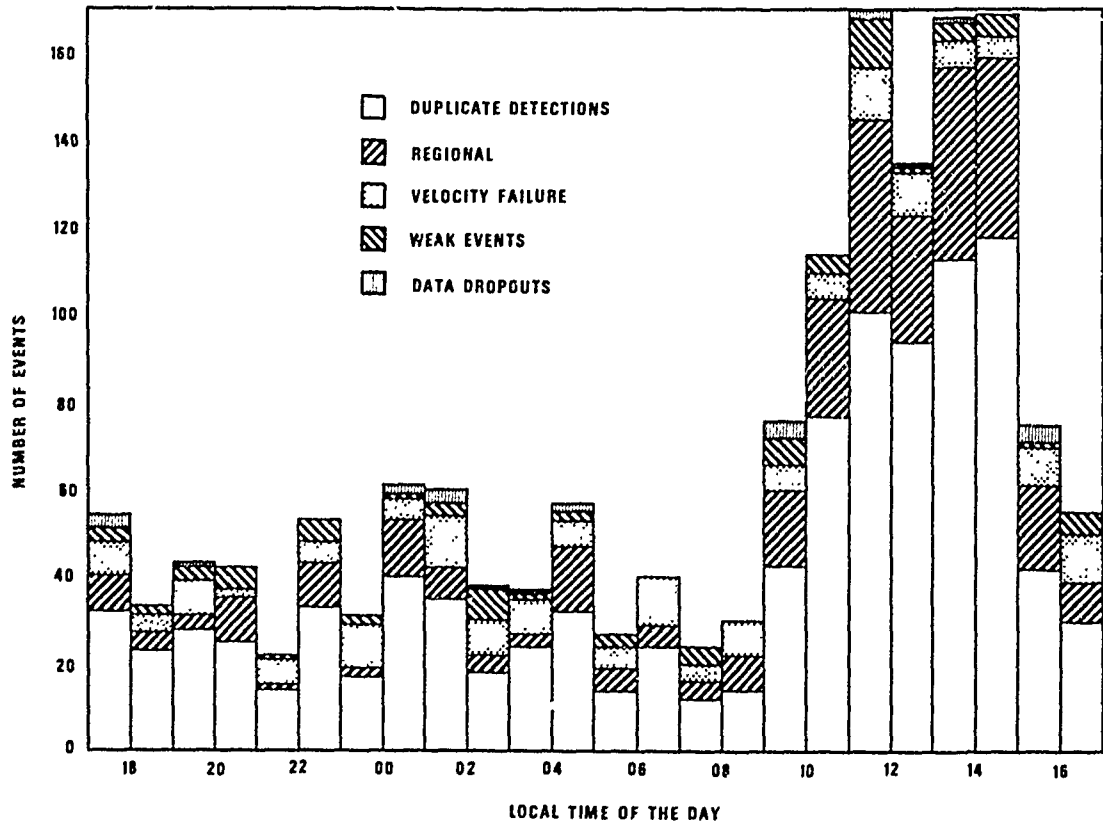


Figure 2b. Diurnal distribution of EP false alarm for LBS133.

showed that both duplicate detections and regional-local events are highly concentrated in the local daytime period from 0800 to 1600 hours. The close correlation of both categories indicates both are due to close range events, giving us the first concrete evidence of the relation between these two categories of false alarms. In order to reduce the number of these false alarms it will be necessary to develop some method for monitoring nearby events.

The remaining question is the cause of the high concentration of close range events in the local daytime. From our experience in operating LASA we know local mining activities can generate signals that result in detections. However, whether the local seismic areas such as Yellowstone Park area or coastal areas of Oregon-California are seismically more active during the daytime is not known. Since the signal detection is based on S/N ratio, more signals are detected during the quiet nighttime than noisy daytime (Chang and Seggelke, 1975). This effect is demonstrated in the diurnal distribution of confirmed events shown in Figure 2a. In this figure the rate of confirmed events is higher during local nighttime, which is in agreement with the result of Chang and Seggelke that showed an excellent correlation of the rate of confirmed events with the hourly noise level. We do not assume that the overall seismicity within the surveillance range of LASA shows diurnal variations as was suggested by Shimshoni (1971) and was criticized by Flinn et al. (1972).

What remains to be clarified is whether particular local areas do or do not have diurnal seismicity changes that can be related to the sharp increases in both regional-local events and duplicate detections during daytime. In Figure 3a we have plotted the number of daily occurrences of duplicate detections and regional-local events during 0800 and 1600 hours. This figure shows

Chang, A. C. and Seggelke, R. M., 1975, The effect of band pass filters on LASA detection performance: SDAC-TR-75-9, Teledyne Geotech, Alexandria, Virginia.

Shimshoni, M., 1971, Evidence for higher seismic activity during the night: Geophys. J. R. Astr. Soc., v. 24, p. 97-99.

Flinn, E. A., R. R. Blandford, and H. Mack, 1972, Comments on "Evidence for higher seismic activity during the night" by Michael Shimshoni: Geophys. J. R. Astr. Soc., v. 28, p. 308-309.

that these two categories are low during weekends and holidays, suggesting that local disturbances are the result of man-made activities, and are not due to diurnal seismicity variations.

It is also likely that codas from local man-made activities will raise the ambient noise level and somewhat impair the detection capabilities of teleseismic signals. In Figure 3b we have plotted the number of daily occurrences of identified events and identified later phases during 0800 to 1600 hours. A good inverse correlation can be found between Figures 3a and 3b in that the number of identified events is higher on Saturdays and Sundays. This result coincides with the work of Woolson (1976) which shows that LASA's detection threshold (90% confidence level) is approximately 0.15 m_b better on Sundays when compared to the same threshold for weekdays. This analysis clearly shows that local cultural activity is a major problem in the LASA's detection performance; it raises the rate of false alarms and lowers its detection capabilities.

Woolson, J., 1976, LASA detection threshold for 1974; Comparison of Monday through Saturday with Sunday: Internal Memorandum, Teledyne Geotech, March 1976.

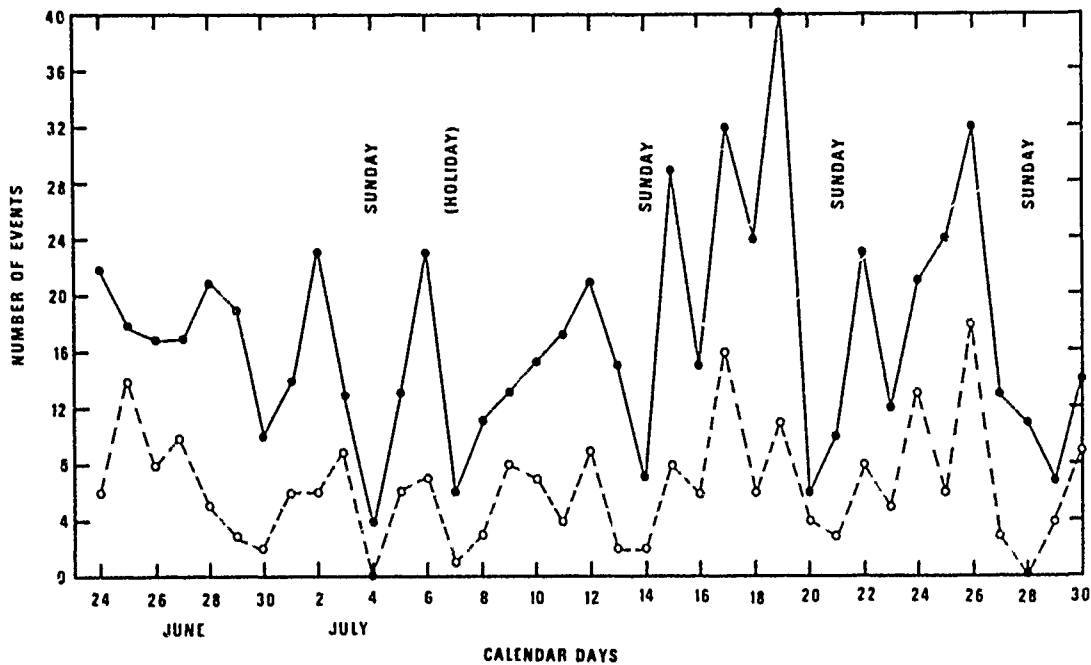


Figure 3a. Number of duplicate detections (open circles) and regional-local events (closed circles) at LASA during daytime (0800-1800 local time) from 24 June to 30 July 1974.

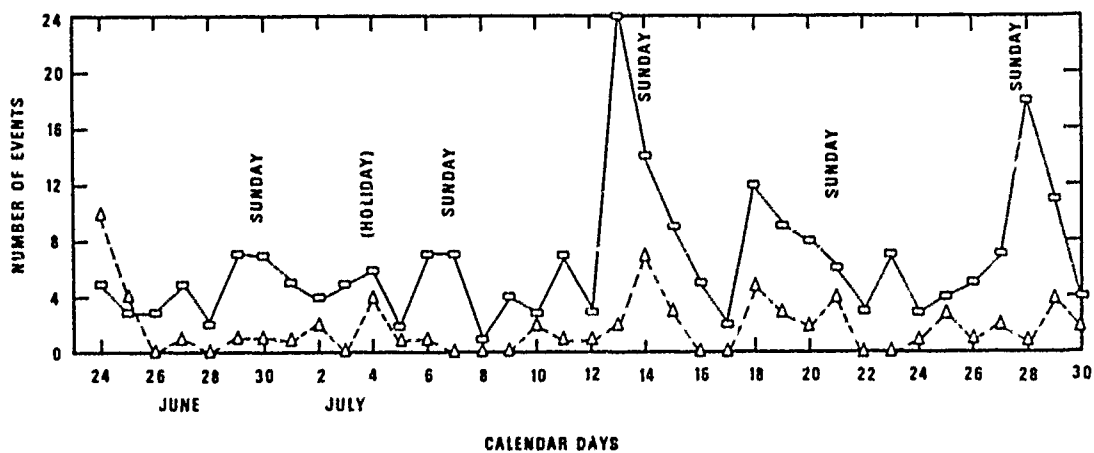


Figure 3b. Number of identified events (squares) and identified later phases (triangles) at LASA during daytime (0800-1600 local time) from 24 June to 30 July, 1974.

DISCUSSION

The good correlation between the daily occurrences of duplicate events and regional-local events shown in Figure 3a indicates that duplicate events result mostly from regional-local disturbances. A good reason for this is that there are no regional-local beams in this beam set. Because regional-local events are generally associated with large amplitudes, misaligned signals are detected on teleseismic beams as side lobe detections and coda detections.

Because the real interest in detecting and locating events with large arrays is in the teleseismic range, and also because of operational difficulties associated with detecting and locating close range events, past operation with LASA has not used beams aimed at local areas. Regional and local events arrive at LASA with relatively low apparent phase velocity, and many beams will be required to maintain adequate surveillance. Even if the signal were correctly detected, because of its high frequencies and changing signal characteristics from subarray to subarray, it would be difficult to locate the event correctly. The mission of the array, computational time and core requirements, and geophysical difficulties, discourage attempts to treat regional-local events. These are the reasons why the DP beam set, LBS133, does not have any beams within 23 degrees of LASA.

However, the results of our analysis in the previous section showed that one way to reduce the false alarm rate is to eliminate local and near regional events. Without beams in close range areas these signals are detected on teleseismic beams and cause and increase in the number of false detections. The fact that we cannot escape detecting local events leads us to argue that perhaps local areas need to be monitored by several DP beams. By detecting signals on close-in beams, side lobe detections in teleseismic beams can be identified and discarded. Since locating nearby events is difficult, a simple algorithm may be devised to eliminate them from further processing by limiting EP to teleseismic signals.

Adding near distance beams to the existing beam set may exceed the computational and core limits in the computer, and this aspect must be discussed before the implementation. The old concept applied to the LBS133 was to deploy beams to known seismic areas with equal beam separation in a hexagonal pattern so that any signal from a seismic area will be detected in one of these beams.

The consequence of rigidly adhering to a pattern is that few of these beams are exactly placed on the known seismic areas, thus all DP detections are made with initial location errors. If DP beams are selected on the basis of world seismicity and are aimed directly at these areas, the required number of DP beams can be reduced and the initial location accuracy can be increased. To avoid missing events from non-seismic areas, coarsely spaced beams can be applied as a safety precaution. The saving in the required number of beams can be used for local beams to reduce the number of false alarms.

In general, side lobe detections will occur when the peak half-cycle on one instrument is added to the following or preceding peak on another instrument in the beamforming process. This type of false alarm will occur within one or two cycles of the main peak of the signal. Since teleseismic signals are known to have a dominant frequency near 1 Hz, side lobe detections occur within one or two seconds of the main detection. A detection algorithm with spatial and temporal constraints of three consecutive threshold crossings will eliminate this type of false alarm. However, during the analysis we found another kind of large scale side lobe detection associated with large signal arrivals. Suppose as an example a large signal has just arrived at the northern most subarray. At this instant this data is being used to form beams aimed toward the south; thus a large signal in one subarray, even when reduced by a factor of N because it is not present on the remaining subarrays, will produce a false detection and may be reported as an event arriving from the south. Since this false detection is spatially and temporarily separated from the main detection, it may appear as a near simultaneous arrival of two independent events from opposite directions. Similar detections can be observed after a large signal has already passed through the array except for one or two subarrays at the edges. The result of a large signal arrival from the north is a set of three detections in south-north-south beams with a few seconds separation. For an array with 50 km in diameter and a large signal with an apparent velocity of 15 km/sec = 3.3 seconds before and after the main detection. Since side lobes are much smaller than the main detection this spurious detection pattern can occur only with a large signal. We think that the pattern of detections, the size of the main detection, and time constraints can be programmed to eliminate this kind of false alarm.

EVALUATION OF THE NEW BEAM SET

In consideration of the reasons discussed in the previous section, a new beam set was designed and tested with the on-line DP for the data from the period of June 13 to June 30, 1975. In this section we analyzed and compared the performance of this new beam set, LBS160, with the old beam set LBS133.

The new beam set has a total of 183 teleseismic beams aimed at locations for which we have LASA travel time corrections (Chiburis and Ahner, 1973). Since these locations are calibrated for travel time corrections, we expect these beams will have minimal signal losses due to travel time errors. In addition, 60 close distance beams and 14 high velocity beams were selected on the basis of regional and PKP-range seismicity. For the purpose of covering non-seismic areas and detecting rare events, 84 beams are added to the beam set. As a result LBS160 has a total of 341 beams compared to 300 beams in the LBS133. Figure 4 shows the distribution of LBS160 beam locations. Detailed beam parameters are given in Appendix A.

All EP signals which were processed during the period of LBS160 operation were analyzed and compared in the same way as the previous analysis. The summary of signal classifications are given in Table II. Comparing the respective categories in Table I, we find that the percentage of the identified events has increased from 33% to 42% of the total, and Duplicate detections have decreased from 36% to 30%. There is an increase from 11.6% to 13.4% in the regional-local events presumably because the new beam set has a better detection capability in close range events.

Next we conduct a recount of all EP signals shown in Table II with a restriction of 10 km/sec to reject all regional-local detections. This restriction eliminates all signals detected within 20 degrees from LASA. The result showed 21 identified events, 161 duplicate detections, 91 regional-local events and 15 weak events were eliminated from processing. Table III shows

Chiburis, E. F. and R. O. Ahner, 1973, LASA regional travel time corrections and associated nodes: SDAC-TR-73-6, Teledyne Geotech, Alexandria, Virginia.

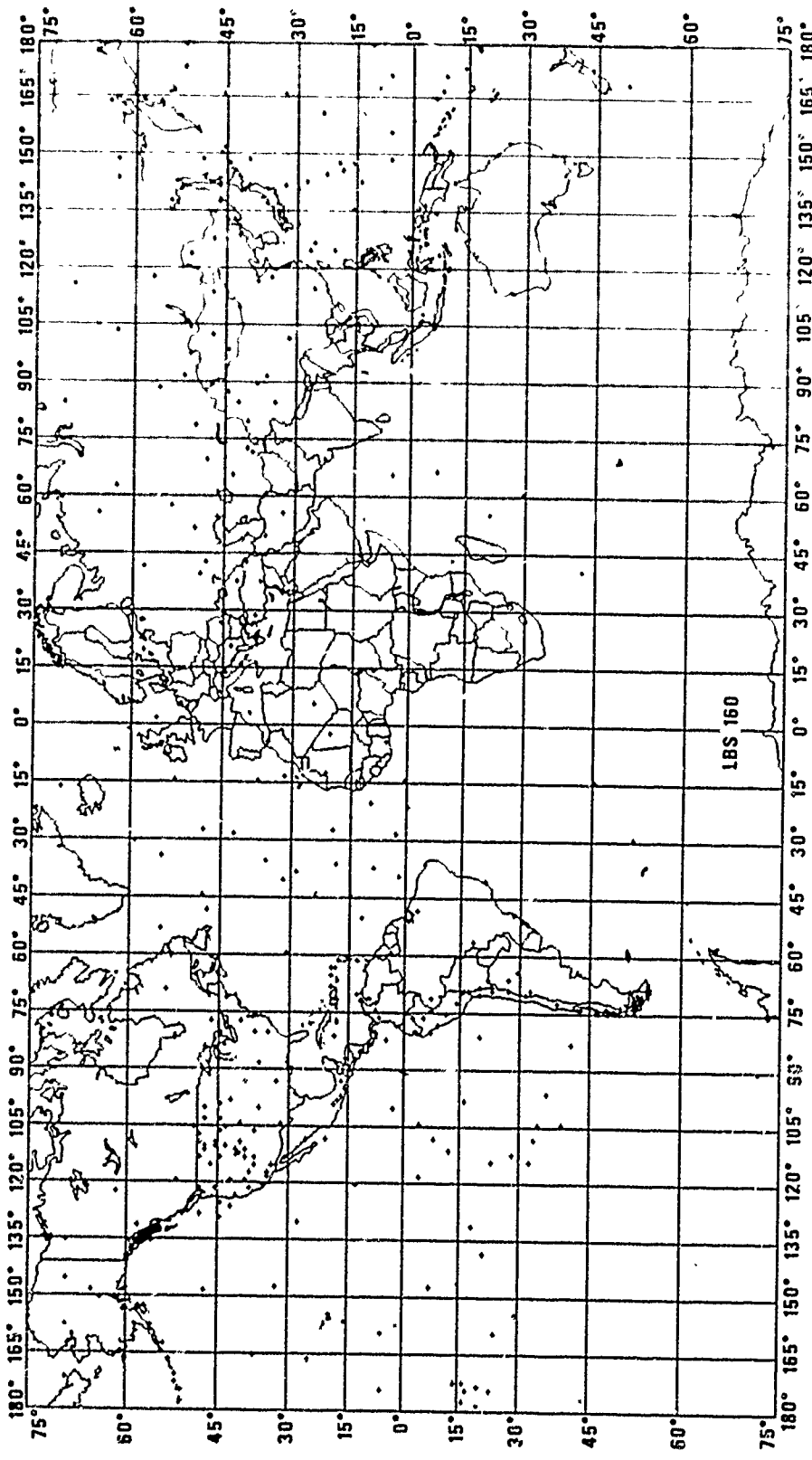


Figure 4. World map showing locations of LBS160 beams.

TABLE II
 Classification of EP Events from June 13 to June 30, 1975
 (Beam Set LBS*160)

Category	Number of Events	%
(1) Identified events	599	42.4
(2) Identified secondary phases	87	6.2
(3) Duplicate detections	422	29.9
(4) Regional or local events	189	13.4
(5) Velocity failures	55	3.9
(6) Weak signals	30	2.1
(7) Data dropouts	<u>29</u>	<u>2.1</u>
Total	1411	100.0

*LBS = LASA Beam Set

TABLE III

Classification of EP Events from June 13 to June 30, 1975
with 10 km/sec Velocity Restriction

Category	Number of Events	%
(1) Identified events	578	51.5
(2) Identified secondary phases	87	7.8
(3) Duplicate detections	261	23.2
(4) Regional or local events	98	8.7
(5) Velocity failures	55	4.9
(6) Weak signals	15	1.3
(7) Data dropouts	<u>29</u>	<u>2.6</u>
Total	1123	100.0

the percentage distribution of each signal category. Comparing respective categories in Table II, we find the percentage of identified events showed an increase from 42.4% to 51.5%. There are also marked reductions in false alarms; duplicate detection from 29.9% to 23.2%, regional-local events from 13.4% to 8.7%, and weak events 2.1% to 1.3%. The result proves that the velocity restriction is indeed a very effective criterion to reduce false alarms.

Although this velocity restriction had eliminated a total of 267 false alarms, it had also eliminated 21 good local events. Among these 21 events, we found one signal detected at 16.5 dB, three detections between 18 to 20 dB, and 17 remaining events with better than 20 dB S/N detection. It is therefore possible to set a higher threshold at about 18 dB to process local detections occurring within 20 degrees from LASA.

By excluding local events there are a total of 578 teleseismic events during the 17 day period, or an average of 34 events per day. This is the highest daily average we have ever obtained at SDAC. In Figure 5, recurrence curves for LBS160 are shown together with similar curves for LBS133 computed for the year 1973. There are a total of 8197 events during 334 days of 1973, or a daily average of 24.5 events per day. Detection thresholds for these two recurrence curves were computed with two methods: the first with the maximum likelihood method by Ringdal (1975), and another by fitting a best linear line estimate between magnitude ranging from 3.8 to 4.9 m_b . By using the maximum likelihood method, 90% detection thresholds does not change much, $m_b = 3.88$ for LBS133 and $m_b = 3.84$ for LBS160. However, the 90% detection thresholds are quite different if we fit a straight line only to the upper portion of the recurrence curve. We find $m_b = 3.8$ for LBS133 and $m_b = 3.55$ for LBS160. It can be seen in Figure 5 that the maximum likelihood method has a better fit over wide range of magnitudes, but the linear line estimate is better for the specified range. We think the true detection threshold change lies somewhere between these two values. Since local events are

Ringdal, F., 1975, On the estimation of seismic detection thresholds: Bull. Seism. Soc. Am., v. 65, p. 1631-1642.

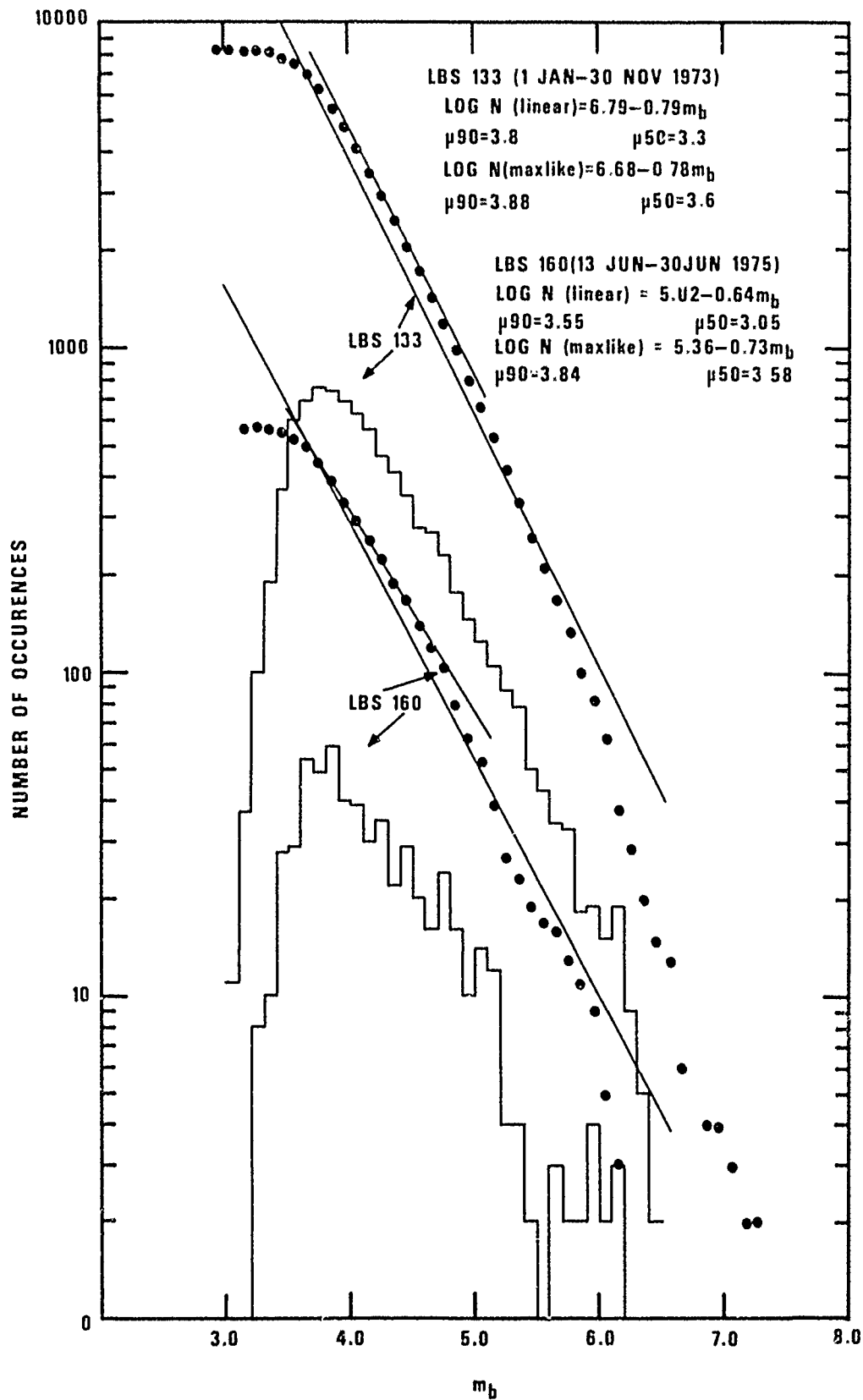


Figure 5. Comparison of recurrence curves computed for LBS133 and LBS160.

excluded in this comparison, we conclude that there is some indication that the more accurate and well calibrated teleseismic beams have improved detection capability by the order of $0.1 \pm .1 m_b$.

Figure 6 shows the performance of LBS160 in terms of percentage distribution of EP signals grouped in the seven categories specified earlier as a function of incremental S/N threshold. The most significant improvement in this figure is the disappearance of regional-local events in high S/N ratio detections. This means that although difficulties with small signals still exist, most of large local events can be properly processed and identified.

The accuracy of the teleseismic beams can be evaluated by comparing travel time errors of the DP beams. The travel time errors are differences of the final travel times of identified events (i.e., the travel time associated with the final location) and travel times of the DP beam which detected the signal. Smaller travel time errors indicate DP beams are more accurate and thus associating DP detections with another station will be optimized. Figure 7 shows the comparison of travel time error is -14.385 seconds for LBS133 and -3.733 for LBS160. Standard deviations are 28.56 for LBS133 and 22.96 for LBS160. An obvious skewness can be observed in the distribution curve of LBS133, but no obvious skew can be seen for LBS160. We believe LBS160 is generally superior to LBS133.

In summary there are three reasons that implementation of new beam set and false alarm criteria will lead to improve performance at LASA. The first reason is the reduction of travel time errors in the new beam set. The mean travel time error for the old beam set is ~14 seconds, which is equivalent to an average initial location error of 200 kilometers at $\Delta = 65$ degrees. The mean travel time error for the new beam set is ~4 seconds and that is equivalent to an average initial location error of 50 kilometers at the same distance. Secondly, new beam locations are well calibrated for travel time anomalies and may well therefore have a lower detection threshold. Thirdly, the reduction of false alarms can reduce the computer-analyst workload so that we can lower the operating threshold without difficulties.

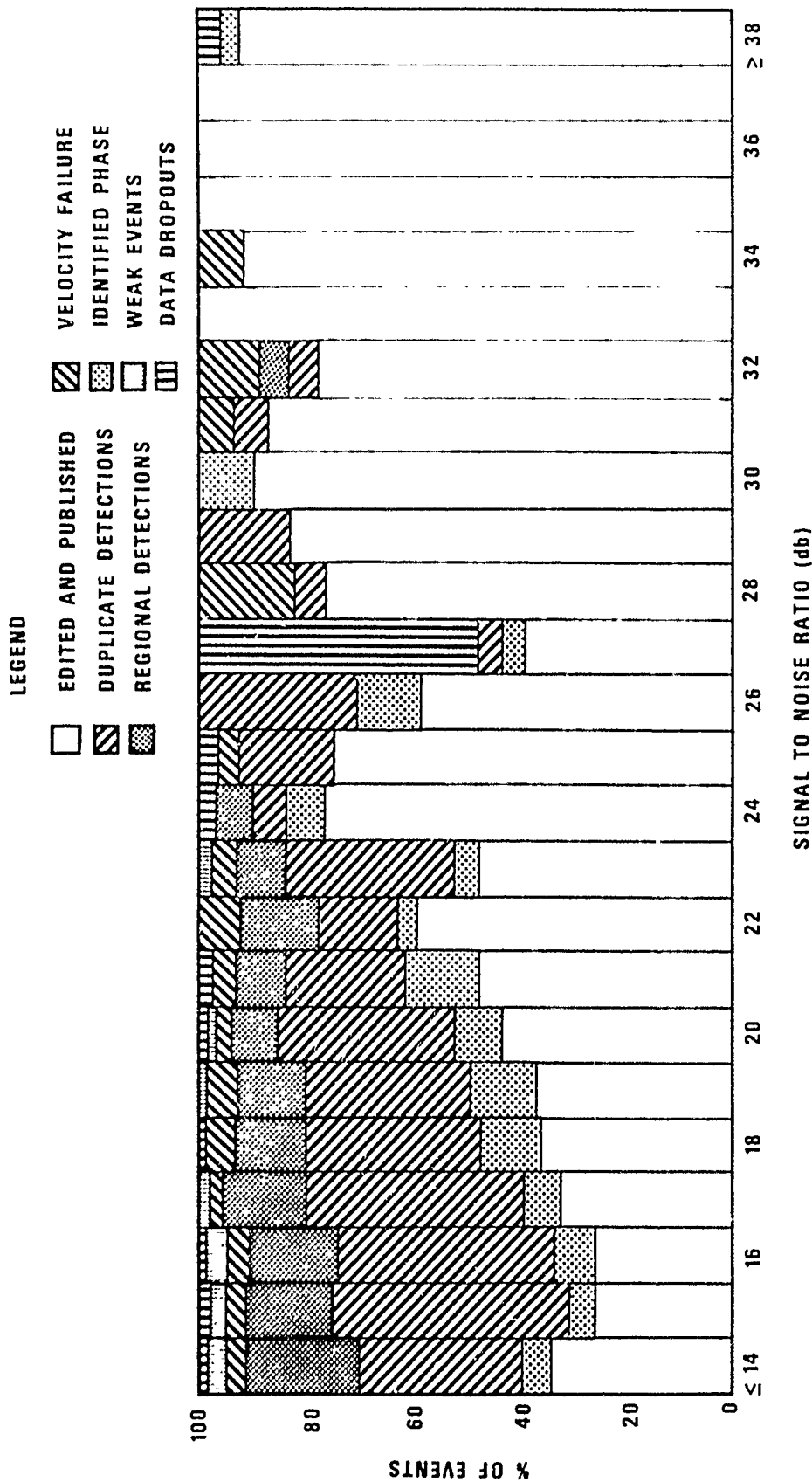


Figure 6. Percentage distribution of EP signals in increments of S/N ratios for the period from 13 June to 30 June 1975 when LBS160 was operational.

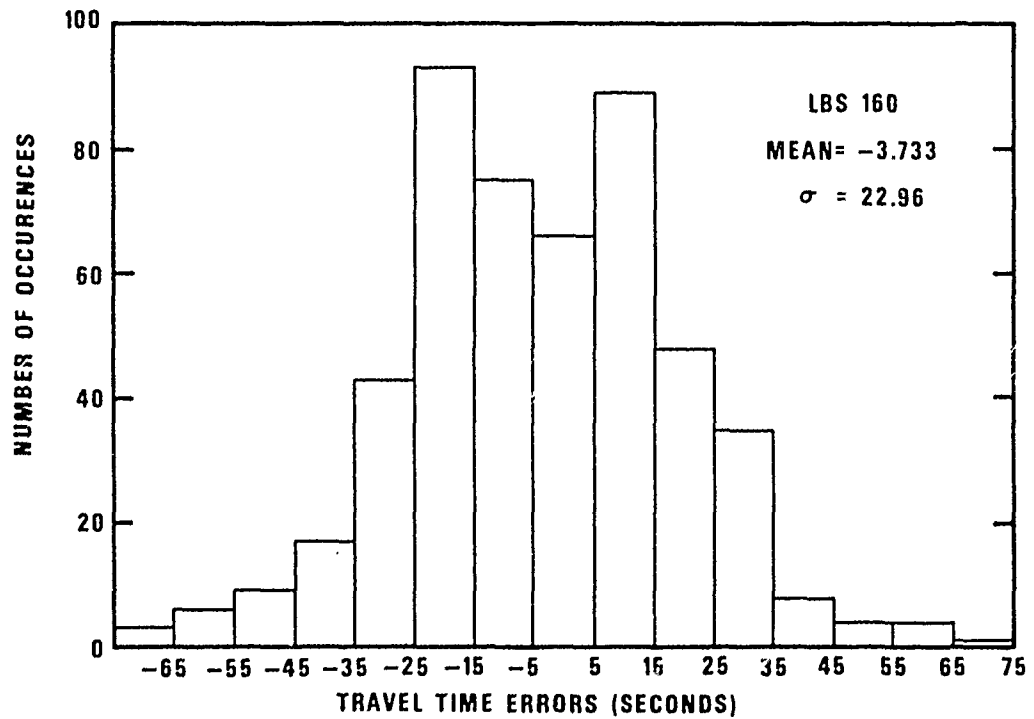
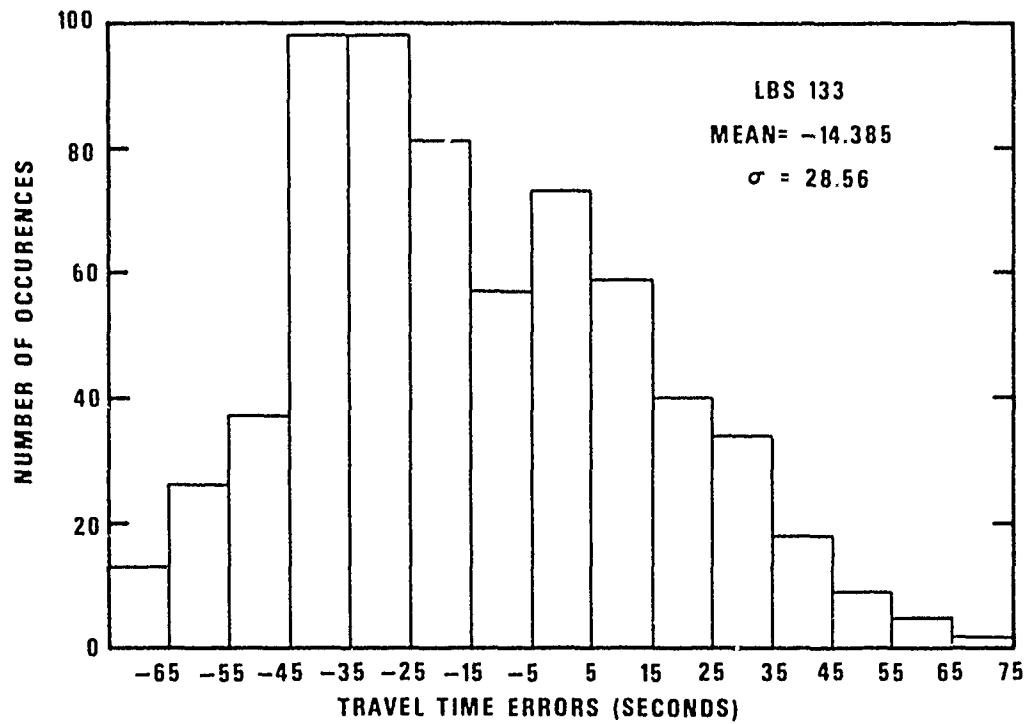


Figure 7. Comparison of travel time errors for LBS133 beams and LBS160 beams.

CONCLUSIONS

As a result of investigating on-line seismic signal detections, we found that seismic signals from local and regional events cause most false alarms, and seismic noise causes few false alarms. Coda from these close range events also disturb the detection capability of the array by masking small teleseismic signals.

Local and near regional events are technically difficult to confirm; however, we found that steering beams to close range areas somewhat reduces the rate of false alarms. In order to discriminate against local events, detection beams must be deployed into these areas. This arrangement will reduce side lobe detections and coda detections on teleseismic beams.

Although the deployment of local beams alone can reduce false alarms, we found the most effective criterion is to set a velocity restriction to eliminate these signals detected on local beams. Since most local events are detected with high S/N ratios, an arrangement to set a high S/N threshold on local beams will pass good events and eliminate false alarms.

Instead of using several beams equally spaced in a particular seismic area, we found it more effective to place one beam directly on the center of the area. Comparison of recurrence curves showed that such a new beam set has a lower detection threshold. This is perhaps due to two factors; detection beams are closer to true epicenters (thus less beamforming loss), and these beams are well calibrated for travel time anomalies for the particular areas used. Deployment of new seismic beams showed that the average location errors of DP detections are reduced from 200 km to 50 km.

ACKNOWLEDGEMENTS

We wish to thank Drs. R. R. Blandford and J. H. Goncz for reviewing this report and offering valuable suggestions.

REFERENCES

- Bungum, H. and F. Ringdal, 1974, Diurnal variation of seismic noise and its effect on detectability: NORSAR Scientific Report No. 5-73/74, NTNF/NORSAR, Kjeller, Norway.
- Bungum, H. and E. S. Husebye, 1974, Analysis of the operational capabilities for detection and location of seismic events at NORSAR: Bull. Seism. Soc. Am., v. 64, p. 637-656.
- Chang, A. C., 1974, A comparison of the LASA-NORSAR short-period arrays: SDAC-TR-74-5, Teledyne Geotech, Alexandria, Virginia.
- Chang, A. C. and R. M. Seggelke, 1975, The effect of band pass filters on LASA detection performance: SDAC-TR-75-9, Teledyne Geotech, Alexandria, Virginia.
- Chiburis, E. F. and R. O. Ahner, 1973, LASA regional travel time corrections and associated nodes: SDAC-TR-73-6, Teledyne Geotech, Alexandria, Virginia.
- Dean, W. C., 1972, A geophysical evaluation of the short-period LASA/SAAC system: SAAC Technical Report No. 5, Teledyne Geotech, Alexandria, Virginia.
- Flinn, E. A., R. R. Blandford, and H. Mack, 1972, Comments on "Evidence for higher seismic activity during the night" by Michael Shimshoni: Geophys. J. R. Astr. Soc., v. 28, p. 308-309.
- Lacoss, R. T., 1972, Variation of false alarm rates at NORSAR: Semiannual Technical Summary, June 1972, Seismic Discrimination MIT Lincoln Laboratory, Cambridge, Massachusetts.
- Ringdal, 1975, On the estimation of seismic detection thresholds: Bull. Seism. Soc. Am., v. 65, p. 1631-1642.
- Shimshoni, M., 1971, Evidence for higher seismic activity during the night: Geophys. J. R. Astr. Soc., v. 24, p. 97-99.
- Steinert, O., E. S. Husebye, and H. Gjoystdal, 1975, Noise variance fluctuations and earthquake detectability: Geophys. J. R. Astr. Soc., v. 41, p. 289-302.
- Woolson, J., 1976, LASA detection threshold for 1974; Comparison of Monday through Saturday with Sunday: Internal Memorandum, Teledyne Geotech, March 1976.

APPENDIX A

List of Parameters for LBS160

BEAM SET 153, GRID 63 BY 63

DEPLOY. NUMBER	ROW-CULUMBERS	GRID NUMBER	GRID SEC NUMBER	DISPLAY NUMBERS	UX (S/M)	LY (S/R)	P-PHASE	LAT (DEG)	LONG (DEG)	PRIORITY	PHASE VELOCITY	BEAM AZIMUTH	RAISE (DEG)	REZIDY INDEX
1	21,28	92	27, 1	0, 2	-0.13500	P	49N	106W	1	7.4574	300.500	1.9.	456	
2	21,18	594	17, 9	0.053845	-0.098076	P	61E	123W	1	8.9378	311.232	17.5.	679	
3	21,35	803	34, 12	-0.038907	-0.086643	P	65N	85W	1	10.5288	24.182	21.54	679	
4	21,10	842	9, 13	0.093005	-0.081123	P	48N	109W	1	8.1328	311.096	2.50	456	
5	21,28	860	27, 13	-0.000847	-0.080387	P	76N	105W	1	12.4857	0.6.5	29.41	678	
6	21,14	910	13, 14	0.070838	-0.074476	P	58N	132W	1	9.7291	316.434	19.71	23	
7	21,28	924	27, 14	-0.000338	-0.076843	P	83N	105W	1	13.0135	0.252	36.45	634	
8	21,24	920	23, 14	0.017165	-0.077372	P	76N	134W	1	12.6177	347.491	31.58	675	
9	21,32	928	31, 14	-0.024713	-0.075256	P	74N	70W	1	12.6247	18.179	31.69	681	
10	21,21	981	20, 15	0.037673	-0.073562	P	57N	135W	1	12.0996	332.881	25.76	677	
11	21,23	983	22, 15	0.028561	-0.072400	P	74N	155W	1	12.8485	338.471	34.66	675	
12	21,28	988	27, 15	-0.001770	-0.070450	P	87N	55E	1	14.1900	1.439	46.62	644	
13	21, 8	1032	7, 16	0.101493	-0.067920	P	52N	120W	1	8.1885	303.791	9.97	23	
14	21,19	1043	18, 16	0.043600	-0.065290	P	67N	159W	1	12.7373	326.265	33.20	676	
15	21,10	1043	18, 16	0.042240	-0.068120	P	67N	148W	1	12.4761	328.198	29.05	676	
16	21,25	1050	25, 16	0.000030	-0.067770	P	92N	119E	1	14.6260	352.410	49.69	654	
17	21,31	1055	30, 16	-0.019060	-0.069280	P	79N	16W	1	13.9171	15.382	44.53	640	
18	21,13	1101	12, 17	0.076188	-0.061905	P	55N	135W	1	10.1867	309.095	20.78	19	
19	21,16	1104	15, 17	0.064787	-0.064145	P	59N	138W	1	10.9686	314.714	22.50	19	
20	21,19	1107	18, 17	0.049350	-0.063130	P	64N	149W	1	12.4797	321.984	29.21	1	
21	21,20	1108	19, 17	0.042130	-0.062490	P	67N	172W	1	13.2687	326.012	38.84	672	
22	21,23	1111	22, 17	0.025226	-0.061255	P	71N	142E	1	15.0951	337.617	53.01	670	
23	21,24	1112	23, 17	0.013315	-0.062122	P	73N	125E	1	15.4402	343.573	55.31	653	
24	21,23	1115	27, 17	0.000017	-0.062440	P	74N	75E	1	15.7768	359.627	58.60	649	
25	21,20	1117	28, 17	-0.000650	-0.061370	P	73N	95E	1	16.1478	0.104	59.63	648	

LTP 116 REGICN CORRECTIONS (ANVER - CHIBUKIS) 191 VODES (JUL 1974)

DEPLOY. NUMBER	ROW-COL NUMBERS	GRID SEQ NUMBER	DISPLAY NUMBERS	UX (S/KM)	UY (S/KM)	PHASE (DEG)	LAT (DEG)	LONG (DEG)	PRIORITY	PHASE VELOCITY	BEAM AZIMUTH	RANGE (DEG)	RECEIVE INDEX
26	21,31	1119	30,17	-0.017160	-0.0264680	P	76.1	15E	1	14.9449	14.842	51.97	643
27	21,33	1121	32,17	-0.027150	-0.062270	P	71.4	2W	1	14.7626	23.623	51.60	639
28	21,17	1163	16,18	0.055570	-0.057740	P	51.4	151W	1	12.4862	316.133	29.45	2
29	21,17	1169	16,18	0.052540	-0.060330	P	63N	151W	1	12.4999	318.948	29.80	1
30	21,24	1176	23,18	0.017630	-0.057673	P	67.4	115E	1	16.5763	343.227	62.39	726
31	21,27	1179	26,18	0.008305	-0.058370	P	68N	84E	1	17.0856	355.782	65.38	725
32	21,31	1183	30,18	-0.018297	-0.057030	P	66N	32E	1	16.6963	17.787	63.14	724
33	21,34	1186	33,18	-0.035190	-0.060500	P	68N	17W	1	14.2878	30.184	47.31	637
34	21, 7	1223	6,19	0.110996	-0.053740	P	48N	110W	1	8.1089	295.834	3.10	455
35	21,17	1233	16,19	0.058680	-0.054530	P	60N	152W	1	12.5064	312.998	29.95	2
36	21,17	1233	16,19	0.057620	-0.055260	P	60N	154W	1	12.5475	313.698	30.60	2
37	21,17	1233	16,19	0.057410	-0.056160	P	60N	149W	1	12.4516	314.369	28.28	14
38	21,20	1236	19,19	0.040488	-0.054738	P	63N	163E	1	14.6877	323.511	50.13	671
39	21,21	1237	20,19	0.034805	-0.053645	P	62N	148E	1	15.6380	327.024	56.50	671
40	21,22	1238	21,19	0.032880	-0.053330	P	62N	143E	1	15.9614	328.344	58.50	671
41	21,25	1241	24,19	0.013862	-0.054489	P	62N	103E	1	17.7859	345.727	69.10	726
42	21,29	1245	28,19	-0.005560	-0.054373	P	52N	02E	1	18.2962	5.839	71.24	335
43	21,30	1246	29,19	-0.008440	-0.055760	P	64N	55E	1	17.7382	8.610	68.92	335
44	21,35	1252	35,19	-0.042270	-0.056110	P	64N	22W	1	14.2349	36.992	46.90	637
45	21, 7	1287	6,20	0.104654	-0.051203	P	51N	129W	1	8.5831	296.071	15.96	22
46	21,15	1295	14,20	0.064250	-0.047620	P	57N	153W	1	12.5042	326.544	29.89	13
47	21,15	1296	15,20	0.056120	-0.050860	P	58N	154W	1	12.5656	309.723	30.86	12
48	21,23	1303	22,20	0.022010	-0.050470	P	57N	117E	1	19.1618	336.438	70.73	328
49	21,25	1306	25,20	0.007190	-0.050244	P	56N	88E	1	19.7522	351.856	76.99	326
50	21,25	1306	25,20	0.001130	-0.047430	P	52.1	91E	1	20.7036	349.104	80.44	325

DEPLOY NUMBER	ACK-COL NUMBERS	GRID SFU NUMBER	DISPLAY NUMBERS	UX (S/NM)	LY (S/KM)	PHASE	LAT (DEG)	LONG (DEG)	PRI- RITY	PHASE VELOCITY	DEAM AZIMUTH	RANGE (DEG)	RESID- INDEX
5	21.29	1369	28.20	-0.008610	-0.048786	P	54N	57E	1	20.1857	15.009	78.67	335
52	21.31	1311	30.20	-0.001026	-0.051990	P	58N	41E	1	19.6515	17.694	72.03	744
53	21.33	1313	32.20	-0.027562	-0.051913	P	58N	19E	1	17.2414	28.372	66.25	537
54	21.35	1315	34.20	-0.037260	-0.048610	P	55N	1E	1	16.3272	37.470	60.76	534
55	21.37	1317	36.20	-0.051640	-0.049780	P	59N	31W	1	13.9418	46.551	44.74	402
56	21.49	1329	48.20	-0.112234	-0.051311	P	47N	104W	1	8.1033	65.431	1.90	461
57	21.10	1360	15.21	0.062910	-0.044650	P	55N	153W	1	12.8627	305.365	35.94	10
58	21.16	1360	15.21	0.063850	-0.046130	P	56N	158W	1	12.6951	305.847	32.72	12
59	21.19	1363	18.21	0.045750	-0.044180	P	53N	159E	1	15.7233	314.000	57.06	219
60	21.19	1363	18.21	0.046240	-0.046870	P	56N	163E	1	15.1883	315.387	53.65	218
61	21.19	1363	18.21	0.048890	-0.045510	P	54N	165E	1	15.0460	312.634	52.69	4
62	21.23	1367	22.21	0.026297	-0.045774	P	51N	123E	1	18.9428	330.123	73.80	658
63	21.24	1368	23.21	0.021146	-0.043310	P	47N	113E	1	20.7470	333.377	80.56	334
64	21.25	1369	24.21	0.014860	-0.043200	P	47N	107E	1	21.8893	341.019	83.85	334
65	21.25	1369	24.21	0.016440	-0.046910	P	52N	135E	1	20.1110	340.632	78.42	327
66	21.25	1370	25.21	0.012320	-0.046240	P	51N	97E	1	20.8973	345.061	81.06	333
67	21.25	1370	25.21	0.027972	-0.043514	P	47N	39E	1	22.6049	349.618	85.75	332
68	21.28	1372	27.21	0.022190	-0.045760	P	50N	78E	1	21.8568	357.256	83.78	329
69	21.28	1372	27.21	0.024487	-0.044264	P	48N	69E	1	22.5561	3.216	85.60	713
70	21.30	1374	29.21	-0.010413	-0.042794	P	46N	54E	1	22.7051	13.676	86.08	336
71	21.30	1374	29.21	-0.11730	-0.045610	P	50N	51E	1	21.2340	14.423	82.13	336
72	21.30	1374	29.21	-0.011972	-0.045819	P	50N	51E	1	21.0933	14.625	81.69	336
73	21.31	1375	30.21	-0.021045	-0.044276	P	48N	42E	1	21.0933	20.943	81.69	357
74	21.32	1376	31.21	-0.018531	-0.044910	P	49N	34E	1	20.5832	22.422	80.51	357
75	21.17	1381	36.21	-0.047445	-0.043325	P	53N	15W	1	15.4417	47.290	55.34	402

DEPLOY. NUMBER	SON-DUL NUMBERS	GRID SEQ NUMBER	DISPLAY NUMBERS	UX (S/KM)	UY (S/KM)	P-HASE	LAT (DEG)	LONG (DEG)	PRIORITY	PHASE VELOCITY	BEAM AZIMUTH	RANGE (DEG)	REDIJA INDEX
76	21,13	1383	38,21	-0.057150	-0.044260	P	55N	35W	1	13.8576	52.367	44.04	402
77	21,14	1385	40,21	-0.065040	-0.044200	P	55N	54W	1	12.7348	55.921	33.25	446
78	21,15	1386	41,21	-0.074079	-0.044629	P	54N	73W	1	11.5629	58.933	24.33	443
79	21,15	1423	14,22	0.062430	-0.039580	P	52N	171W	1	13.5282	32.374	41.24	9
80	21,15	1423	14,22	0.064850	-0.041750	P	54N	153W	1	12.9656	32.773	35.97	17
81	21,15	1423	14,22	0.063760	-0.040220	P	53N	157W	1	13.2651	302.244	38.81	9
82	21,16	1424	15,22	0.059200	-0.039160	P	51N	178W	1	14.0885	333.484	45.87	7
83	21,16	1424	15,22	0.061350	-0.039660	P	52N	173W	1	13.6867	332.894	42.63	7
84	21,16	1424	15,22	0.060950	-0.038510	P	51N	175W	1	13.8784	302.307	44.21	7
85	21,17	1425	16,	0.052990	-0.042150	P	52N	172E	1	14.7758	308.467	50.76	5
86	21,17	1425	16,22	0.057030	-0.040110	P	52N	178E	1	14.3426	335.119	47.69	6
87	21,19	1427	18,22	0.043980	-0.038260	P	45N	151E	1	17.1547	311.021	65.77	221
88	21,19	1427	18,22	0.044960	-0.041820	P	50N	156E	1	16.2859	312.927	60.50	221
89	21,20	1428	19,22	0.037640	-0.040720	P	46N	141E	1	18.0337	317.251	70.22	661
90	21,20	1428	19,22	0.041070	-0.041790	P	49N	135E	1	17.0669	315.498	65.28	663
91	21,21	1429	20,22	0.032630	-0.039310	P	43N	132E	1	19.5740	320.305	76.51	661
92	21,21	1429	20,22	0.035170	-0.040810	P	46N	137E	1	18.5619	319.245	72.28	661
93	21,22	1430	21,22	0.029196	-0.042557	P	47N	127E	1	19.3763	325.548	75.72	658
94	21,22	1430	21,22	0.031448	-0.038637	P	42N	128E	1	20.4050	322.035	79.42	659
95	21,24	1432	23,22	0.018913	-0.039621	P	42N	109E	1	22.7772	334.482	86.31	334
96	21,25	1433	24,22	0.012873	-0.041474	P	44N	98E	1	23.0277	342.756	87.13	334
97	21,25	1434	25,22	0.008710	-0.040160	P	38N	89E	1	24.3346	347.763	94.57	321
98	21,25	1434	25,22	0.006048	-0.039460	P	34N	84E	1	25.0495	351.286	99.50	306
						PP	65S	67E	1	25.0495	351.286	198.54	425
						PKP	40S	75E	1	25.0495	351.286	173.25	429

DEPLOY- NUMBER	ADM-COL NUMBERS	GRID SEC NUMBER	DISPLAY NUMBERS	UX (S/N/Y)	LY (S/N/Y)	PHASE	LAT (DEG)	LONG (DEG)	PRIOR- RITY	PHASE VELOCITY	BLAZ AZIMUTH	RANGE (DEG)	RESIDY INDEX
99	21,25	1434	25,22	0.006920	-0.041910	P	44N	87E	1	23.5419	350.624	89.33	332
100	21,25	1434	25,22	0.005650	-0.041570	P	42N	84E	1	23.8366	352.260	91.11	332
101	21,26	1434	25,22	0.009818	-0.039448	P	36N	91E	1	24.5592	346.023	96.25	325
102	21,27	1435	26,22	0.002630	-0.041230	P	40N	79E	1	24.2050	356.350	93.68	321
103	21,28	1436	27,22	-0.004718	-0.041880	P	43N	65E	1	23.7278	6.428	90.37	713
104	21,28	1436	27,22	-0.000710	-0.041400	P	40N	72E	1	24.1510	0.982	93.32	716
105	21,28	1436	27,22	-0.001630	-0.040980	P	39N	71E	1	24.3829	2.278	94.87	717
106	21,29	1437	28,22	-0.007880	-0.039747	P	36N	60E	1	24.6790	11.214	96.75	341
107	21,30	1438	29,22	-0.013890	-0.039860	P	41N	48E	1	23.6906	19.212	90.12	337
108	21,30	1438	29,22	-0.011081	-0.038349	P	32N	55E	1	25.0512	16.117	99.54	348
						PP	64S	85E	1	25.0512	16.117	198.54	436
						PKP	43S	71E	1	25.0512	16.117	173.25	425
						PKKP	59S	137E	1	25.0512	16.117	108.49	691
						PKPPKP	34N	111E	1	25.0512	16.117	13.49	495
						SCP	68N	33E	1	25.0512	16.117	61.32	724
						SKP	7S	63E	1	25.0512	16.117	139.57	425
						SKKP	78S	129E	1	25.0512	16.117	142.17	729
						AP	32N	55E	1	25.0512	16.117	99.54	348

DEPLOY. NUMBER	ROW-COL NUMBERS	GRID SEQ NUMBER	DISPLAY NUMBERS	UC (S/KV)	UY (S/KV)	PHASE	LAT (DEG)	LONG (DEG)	PRIM-RTY	PHASE VELOCITY	HEAM AZIMUTH	RANGE (DEG)	RESIDV INDEX
109	21,30	1438	29,22	-0.03875	-0.03875	P	32°	20E	1	25.0512	16.117	99.52	348
110	21,31	1439	30,22	-0.03912	-0.03912	P	36°	47E	1	24.3803	19.933	94.87	347
111	21,31	1439	30,22	-0.03912	-0.03912	P	42N	37E	1	22.6337	26.580	85.84	360
112	21,32	1440	31,22	-0.02594	-0.04173	P	43N	42E	1	23.4798	23.893	89.02	366
113	21,33	1441	32,22	-0.03007	-0.03730	P	45N	26E	1	20.3520	31.865	79.24	358
114	21,34	1442	33,22	-0.03411	-0.03969	P	43N	20E	1	20.2084	37.421	78.76	383
115	21,35	1443	34,22	-0.03658	-0.04080	P	44N	13E	1	19.1082	40.676	74.57	545
						P	45N	8E	1	18.4287	42.386	71.75	545
116	21, 5	1477	4,23	0.01178	-0.03549	P	48N	114W	1	8.1266	286.764	5.43	456
117	21,18	1490	17,23	0.05205	-0.03479	P	45N	165E	1	15.9702	303.761	58.56	16
118	21,20	1492	19,23	0.04262	-0.03415	P	40N	148E	1	18.3091	308.730	71.30	229
119	21,20	1492	19,23	0.04200	-0.03754	P	44N	147E	1	17.7523	311.790	68.99	221
120	21,20	1492	19,23	0.03936	-0.03662	P	42N	143E	1	18.6009	312.935	72.43	224
121	21,21	1493	20,23	0.03822	-0.03511	P	40N	141E	1	19.2683	312.571	75.26	227
122	21,23	1495	22,23	0.02377	-0.03497	P	35N	117E	1	23.6462	325.790	89.86	664
123	21,24	1496	23,23	0.02271	-0.03657	P	38N	116E	1	23.2302	328.159	87.96	658
124	21,25	1497	24,23	0.01590	-0.03671	P	31N	101E	1	24.9916	336.575	98.85	307
125	21,31	1501	30,23	-0.01646	-0.03801	P	35N	44E	1	24.1424	23.415	93.25	346
126	21,32	1504	31,23	-0.02246	-0.03452	P	32N	34E	1	24.2816	33.249	94.22	373
127	21,32	1504	31,23	-0.02031	-0.03691	P	37N	37E	1	23.7367	28.822	90.40	374
128	21,33	1505	32,23	-0.02847	-0.03542	P	35N	22E	1	22.0053	38.792	84.14	368
129	21,33	1505	32,23	-0.02476	-0.03626	P	38N	28E	1	22.7753	34.327	86.31	366
130	21,34	1506	33,23	-0.03271	-0.03728	P	41N	15E	1	23.1630	41.264	78.60	390
131	21,39	1511	38,23	-0.05712	-0.03591	P	48N	28W	1	14.8214	57.843	51.09	403
132	21, 6	1542	5,24	0.01162	-0.03057	P	49N	129W	1	8.4990	285.052	15.47	25

DEPLOY. NUMBER	RC-CCL NUMBER	GRID SEL NUMBER	DISPLAY NUMBER	UX (S/KM)	UY (S/KM)	PHASE	LAT (DEG)	LONG (DEG)	POLARITY	PHASE VELOCITY	BEAM A/WIDTH	RANGE (DEG)	REZID INDEX
133	21.23	1556	19.24	0.027860	-0.032440	P	35.1	140E	1	23.0573	315.591	78.24	228
134	21.23	1556	19.24	0.038060	-0.029370	P	32N	141E	1	22.8010	317.656	80.74	211
135	21.21	1557	20.24	0.031940	-0.030280	P	32N	132E	1	22.7212	313.471	86.12	235
136	21.22	1559	21.24	0.028420	-0.029700	P	25N	124E	1	24.3549	316.281	94.57	245
137	21.23	1559	22.24	0.025721	-0.033598	P	32N	120E	1	23.8566	322.149	91.27	664
138	21.23	1559	22.24	0.02789	-0.032059	P	25N	114E	1	25.0496	323.423	99.50	664
						PP	60S	52E	1	25.0496	323.423	198.54	425
						PKP	61S	79E	1	25.0496	323.423	173.25	429
						PKP	49S	47E	1	25.0496	323.423	108.49	409
						PKPKP	35N	96E	1	25.0496	323.423	13.49	499
						SCP	57N	145E	1	25.0496	323.423	61.32	663
						SKP	11S	37E	1	25.0496	323.423	139.57	425
						SKKP	66S	11E	1	25.0496	323.423	142.17	414
						AP	29N	114E	1	25.0496	323.423	99.50	664
						XP	25N	114E	1	25.0496	323.423	99.50	664
139	21.23	1569	32.24	-0.027580	-0.033480	P	35N	23E	1	23.0537	37.481	87.29	370
140	21.40	1576	39.24	-0.027331	-0.031513	P	48N	45W	1	13.4516	64.918	40.54	402
141	21.5	1605	4.25	0.125047	-0.027713	P	47N	112W	1	8.1166	282.999	4.30	456
142	21.21	1621	20.25	0.037690	-0.025560	P	27N	142E	1	22.5942	303.620	84.36	212
143	21.21	1621	20.25	0.036880	-0.027180	P	29N	140E	1	21.8276	326.389	83.70	211
144	21.22	1622	21.25	0.031280	-0.029100	P	29N	131E	1	23.4066	312.932	88.65	238
145	21.22	1622	21.25	0.024520	-0.028561	P	25N	126E	1	24.3201	313.997	94.46	246
146	21.22	1622	21.25	0.029110	-0.027315	P	25N	124E	1	25.0496	313.176	99.50	248
						PP	57S	49E	1	25.0496	313.176	198.54	425
						PKP	62S	80E	1	25.0496	313.176	173.25	429

DEPLOY. NUMBER	ROW-COL NUMBERS	GRID SEC NUMBER	DISPLAY NUMBERS	UX (S/KV)	UY (S/KV)	PHASE	LAT (D-M-S)	LONG (DEG)	PRIORITY	PHASE VELOCITY	BEAM AZIMUTH	RANGE (DEG)	RESIDUAL INDEX
147	21,37	1637	36,25	-0.022300	-0.029170	P	35N	5W	1	18.5022	57.336	72.04	385
148	21,38	1638	37,25	-0.051913	-0.027558	P	37N	15W	1	17.0144	62.038	64.99	432
149	21,40	1640	39,25	-0.060070	-0.027380	P	42N	29W	1	15.1479	65.496	53.37	404
150	21,41	1641	40,25	-0.070080	-0.029520	P	47N	49W	1	13.1838	67.506	38.06	402
151	21,43	1643	42,25	-0.076980	-0.027534	P	49N	66W	1	12.3166	70.176	26.88	448
152	21, 4	1658	3,26	0.119893	-0.021374	P	48N	122W	1	8.2113	280.103	11.12	29
153	21,13	1677	12,26	0.076873	-0.022738	P	47N	149W	1	12.4742	286.477	29.00	17
154	21,17	1681	16,26	0.053361	-0.021979	P	32N	165E	1	17.3279	292.386	66.74	611
155	21,20	1684	19,26	0.038100	-0.020840	P	22N	144E	1	23.0271	298.678	87.19	215
156	21,21	1685	20,26	0.034442	-0.020921	P	15N	135E	1	24.8150	311.275	97.68	241
157	21,35	1699	34,26	-0.037450	-0.022840	P	24N	5E	1	22.7970	78.622	86.37	551
158	21,37	1701	36,26	-0.051150	-0.022700	P	31N	14W	1	17.8696	66.069	69.53	393
159	21,19	1747	18,27	0.048645	-0.016480	P	23N	150E	1	19.4702	288.715	76.11	611
160	21,20	1748	19,27	0.039360	-0.018280	P	19N	147E	1	23.0426	294.911	87.24	215
161	21,20	1748	19,27	0.038980	-0.015980	P	15N	147E	1	23.7370	292.291	90.43	216
162	21,21	1749	20,27	0.038490	-0.018440	P	18N	145E	1	23.4306	295.598	88.80	216
163	21,21	1749	20,27	0.037410	-0.016790	P	13N	142E	1	24.3873	294.171	94.87	210
164	21,29	1757	28,27	-0.003360	-0.016310	PAP	4N	65E	1	60.0511	111.640	128.60	421

DEPLOY. NUMBER	CH-CUL NUMBERS	GRID SE. NUMBER	DISPLAY NUMBER	UC (S/N)	LY (S/N)	PHASE	LAT (°N)	LONG (°E)	PRIL-RIFY	PHASE VELOCITY	SLAN AZIMUTH	RANGE (DEG)	STATION INDEX
165	21,36	1764	35,27	-0.041646	-0.017744	P	23N	3W	1	22.0904	66.923	84.35	550
166	21,40	1768	39,27	-0.064590	-0.016040	P	35N	35W	1	15.3281	76.951	52.50	493
167	21,43	1776	47,27	-0.162900	-0.017708	P	46N	78W	1	9.5664	90.226	19.36	447
168	21,51	1779	50,27	-0.117977	-0.018620	P	47N	85W	1	8.3726	81.031	14.53	468
169	21,14	1806	13,28	0.079749	-0.012296	P	37N	155W	1	13.9258	279.859	44.60	611
170	21,25	1817	24,28	0.011340	-0.011960	PKPD	7S	104E	1	60.6744	316.524	132.90	273
171	21,28	1820	27,28	-0.033340	-0.015350	PKPD	56N	125E	1	60.6744	316.524	15.35	23
172	21,37	1829	36,28	-0.048449	-0.014715	P	59N	133E	1	60.6744	316.524	20.12	19
173	21,19	1875	18,29	0.044770	-0.008665	P	12N	160E	1	21.9291	280.954	83.95	615
174	21,20	1876	19,29	0.041030	-0.007379	P	5N	155E	1	24.0173	279.789	92.39	614
175	21,20	1876	19,29	0.039065	-0.010435	P	5N	148E	1	24.7314	284.955	97.11	614
176	21,25	1881	24,29	0.015100	-0.007400	PKPD	8S	123E	1	59.4680	296.108	123.28	286
177	21,29	1885	28,29	-0.006030	-0.007440	PKPD	51N	129E	1	59.4680	296.108	15.69	22
						PKPD	52N	137E	1	59.4680	296.108	20.57	21
						PKPD	6S	125E	1	59.4680	296.108	120.37	280
						PKPD	50S	60E	1	101.1049	37.565	160.20	428

DEPLOY. NUMBER	NUM-COL NUMBERS	GRID SEQ NUMBER	DISPLAY NUMBERS	UX (S/KM)	UY (S/KM)	PHASE	LAT (DEG)	LONG (DEG)	PRIORITY	PHASE VELOCITY	BEAM AZIMUTH	RANGE (DEG)	SECTION INDEX
178	21,36	1892	35,29	-0.640382	-0.008274	P	5N	5W	1	24.2593	78.421	94.04	550
179	21,41	1897	40,29	-0.566860	-0.007990	P	31N	41W	1	14.8510	83.185	51.30	403
180	21, 4	1924	3,30	0.122770	-0.004171	P	46N	116W	1	8.1406	271.946	6.75	33
181	21,20	1940	19,30	0.640920	-0.002760	P	1S	158E	1	24.3825	273.858	94.87	191
182	21,24	1944	23,30	0.016220	-0.005320	PKPD	4S	136E	1	58.5817	288.159	112.20	196
183	21,37	1957	36,30	-0.648363	-0.002324	P	49N	130E	1	58.5817	288.159	15.94	25
184	21,38	1958	37,30	-0.556460	-0.005040	P	49N	137E	1	58.5817	288.159	20.91	21
185	21,40	1960	39,30	-0.564910	-0.005990	P	0N	139E	1	58.5817	288.159	106.74	196
186	21,44	1964	43,30	-0.584057	-0.004488	P	9N	21W	1	20.6531	87.249	80.25	402
187	21, 5	1990	5,31	0.115262	-0.001654	P	19N	28W	1	17.6414	64.898	68.43	402
188	21,19	2003	18,31	0.047120	0.000890	P	28N	39W	1	15.3408	84.728	54.67	403
189	21,30	2014	29,31	-0.011720	0.000730	PKPD	43N	72W	1	11.8798	86.944	24.95	476
190	21,35	2020	35,31	-0.042020	-0.000140	P	44N	130W	1	8.6750	270.822	16.43	30
191	21,40	2024	39,31	-0.060040	0.001760	P	5N	170E	1	21.2278	208.917	82.12	615
192	21, 4	2052	3,32	0.121555	0.005405	P	43S	40E	1	85.1592	93.564	155.88	431
193	21, 4	2052	3,32	0.123276	0.002266	P	45N	91E	1	85.1592	93.564	10.73	466
						SCP	44N	87E	1	85.1592	93.564	13.97	468
						PKPD	42S	36E	1	85.1592	93.564	152.62	431
						P	0N	15W	1	23.7980	89.809	90.85	407
						P	184	37W	1	16.6484	91.679	62.84	402
						P	45N	122W	1	8.2186	267.454	11.47	28
						P	47N	111W	1	8.1118	268.947	3.60	456

DEPLOY. NUMBER	RCI-CUL NUMBERS	GRID SEQ NUMBER	DISPLAY NUMBERS	UC (S/N)	LY (S/N)	PHASE	LAT (DEG)	LONG (DEG)	PRIORITY	PHASE VELOCITY	BEAM AZIMUTH	RANGE (DEG)	RCI-CUL INDEX
194	21,15	2053	14,32	0.004300	0.004300	P	24N	167W	1	15.2964	266.538	53.01	612
195	21,17	2055	16,32	0.003165	0.003165	P	15N	178E	1	18.7513	266.597	73.04	615
196	21,22	2069	19,32	0.003890	0.003890	P	7S	164E	1	24.3673	264.556	94.87	183
197	21,20	2068	19,32	0.003370	0.003370	P	7S	166E	1	24.3589	262.484	94.70	183
198	21,36	2084	35,32	-0.003580	0.003610	P	1S	22W	1	22.9680	94.735	86.63	426
199	21,40	2099	39,32	-0.005560	0.003700	P	23N	45W	1	15.2290	93.230	53.92	423
200	21,51	2099	50,32	-0.123255	0.002377	P	47N	101W	1	9.1117	91.105	3.63	461
201	21, 5	2117	4,33	0.119695	0.007859	P	44N	126W	1	8.3366	266.243	14.17	30
202	21,20	2132	19,33	0.000660	0.000140	P	10S	170E	1	24.1157	258.679	93.07	183
203	21,31	2143	30,33	-0.013830	0.009630	PKPD	46S	15W	1	59.3385	124.850	121.92	410
204	21,37	2149	36,33	-0.008260	0.007130	P	24N	29W	1	20.4986	98.404	79.72	426
205	21,39	2151	39,33	-0.005070	0.009350	P	48N	38W	1	17.8694	130.242	69.53	406
206	21,42	2154	41,33	-0.074280	0.011012	P	30N	60W	1	13.3170	98.433	39.24	402
207	21,13	2189	12,34	0.076517	0.013049	P	32N	148W	1	12.8830	260.322	35.05	611
208	21,17	2193	16,34	0.052931	0.011511	P	54N	175W	1	18.4611	257.730	71.84	611
209	21,20	2196	19,34	0.009290	0.011580	P	15S	172E	1	24.4135	253.578	95.03	185
210	21,20	2196	19,34	0.008360	0.015460	P	18S	178E	1	24.1790	248.049	93.50	182
211	21,25	2201	24,34	0.012460	0.011350	PKPD	51S	168E	1	59.3314	227.669	121.92	166
						S-P	35N	120E	1	59.3314	227.669	15.72	39
						PCP	31N	124E	1	59.3314	227.669	20.62	611
						SKPD	49S	173E	1	59.3314	227.669	118.50	168
212	21,30	2206	29,34	-0.011410	0.012510	PKPD	53S	30W	1	59.2603	137.633	118.59	152

DEPLOY. NUMBER	RCM-COL NUMBERS	PART NO. NUMBER	DISP. BY NUMBERS	OR (S/RM)	Y (S/R)	PHASE	LAT (DEG)	LONG (DEG)	PRIORITY	PHASE VELOCITY	BEAM AZIMUTH	RANGE (DEG)	RECORD INDEX
213	21,37	2213	36,34	-0.050923	0.015609	P	16	60W	1	18.7751	107.042	73.15	402
214	21,39	2215	38,34	-0.062213	0.012270	P	14	45W	1	16.2740	101.518	60.42	403
215	21,46	2222	45,34	-0.094254	0.013015	P	60N	78W	1	10.5154	97.866	21.51	473
216	21,6	2246	5,35	0.115060	0.019087	P	42N	127W	1	8.5739	260.581	15.91	30
217	21,20	2260	19,35	0.039190	0.019980	P	15S	173W	1	22.7328	242.986	86.17	173
218	21,21	2261	20,35	0.037770	0.019530	P	18S	175W	1	23.5181	242.657	89.21	173
219	21,21	2261	20,35	0.038430	0.017420	P	17S	178W	1	23.7001	245.615	90.18	181
220	21,21	2261	20,35	0.036770	0.018140	P	21S	179W	1	24.2306	242.994	93.86	181
221	21,37	2277	36,35	-0.045607	0.016057	P	5S	37W	1	20.6822	1.9.396	80.35	528
222	21,15	2319	14,36	0.062870	0.022560	P	15N	157W	1	14.9712	250.260	52.16	612
223	21,15	2319	14,36	0.066140	0.020510	P	17N	155W	1	14.4410	252.771	48.38	613
224	21,20	2374	19,36	0.036500	0.020900	P	21S	174W	1	23.7754	240.204	93.67	173
225	21,20	2324	19,36	0.038150	0.020650	P	17S	173W	1	23.0520	241.574	87.27	174
226	21,21	2325	20,36	0.035320	0.021270	P	24S	175W	1	24.2542	238.943	94.00	175
227	21,34	2338	33,36	-0.035565	0.022729	P	22S	41W	1	23.6922	122.582	90.15	528
228	21,39	2343	38,36	-0.059311	0.020277	P	11N	51W	1	15.9537	100.874	58.46	402
229	21,17	2385	16,37	0.055023	0.025153	P	5N	160W	1	16.5290	245.433	62.09	622
230	21,34	2402	33,37	-0.030600	0.028800	P	27S	50W	1	23.7973	133.263	90.82	528
231	21,37	2405	36,37	-0.048421	0.025368	P	4S	49W	1	18.2936	117.650	71.24	528
232	21,40	2408	39,37	-0.064230	0.028360	P	17N	62W	1	14.2425	113.923	47.00	92
233	21,40	2408	39,37	-0.062473	0.028580	P	15N	61W	1	14.5566	114.584	49.19	92
234	21,21	2453	23,38	0.032005	0.029339	P	25S	150W	1	22.7772	227.164	86.31	632

DEPLOY. NUMBER	ROW-COL NUMBERS	GRID SEQ NUMBER	DISPLAY NUMBERS	UX (S/KY)	UY (S/KY)	P-HASE	LAT (DEG)	LONG (DEG)	PRIORITY	PHASE VELOCITY	BEAM AZIMUTH	RANGE (DEG)	REGION INDEX
235	21,22	2454	21,38	0.228054	0.032552	P	305	155W	1	23.2705	220.755	88.14	632
236	21,34	2466	33,38	-0.035986	0.033701	P	195	57W	1	20.2829	133.122	79.01	528
237	21,33	2471	38,38	-0.059220	0.032190	P	12N	62W	1	14.8361	118.527	51.16	95
238	21,40	2472	39,38	-0.065690	0.032290	P	19N	65W	1	13.6617	116.176	42.41	90
239	21,40	2472	39,38	-0.065680	0.030060	P	19W	64W	1	13.8443	114.592	43.93	91
240	21,40	2472	39,38	-0.064760	0.030930	P	18N	64W	1	13.9340	115.530	44.67	91
241	21,45	2478	57,38	-0.094830	0.030420	P	37N	81W	1	10.0412	107.786	20.45	491
242	21, 5	2502	5,39	0.113184	0.037793	P	41N	124W	1	8.3803	251.535	14.60	35
243	21,31	2527	30,39	-0.017900	0.038040	P	39S	73W	1	23.7863	154.800	90.74	136
244	21,33	2529	32,39	-0.025400	0.036540	P	30S	65W	1	22.4714	145.196	85.35	141
245	21,38	2534	37,39	-0.052311	0.033761	P	3N	60W	1	16.0617	122.838	59.11	528
246	21,40	2536	39,39	-0.064200	0.036420	P	19N	69W	1	13.5481	119.566	41.41	89
247	21,43	2539	42,39	-0.079769	0.036918	P	34N	81W	1	11.3769	114.835	23.55	511
248	21, 6	2566	5,40	0.114172	0.042557	P	42N	120W	1	8.2071	249.557	10.91	32
249	21,19	2579	18,40	0.042076	0.040229	P	8S	148W	1	17.1784	226.286	65.91	632
250	21,30	2590	29,40	-0.011830	0.040430	P	42S	84W	1	23.7387	163.690	90.43	686
251	21,32	2592	31,40	-0.025280	0.040790	P	28S	70W	1	25.8383	148.211	80.87	122
252	21,32	2592	31,40	-0.021970	0.039480	P	32S	71W	1	22.1330	150.905	84.46	135
253	21,32	2592	31,40	-0.021960	0.038250	P	33S	70W	1	22.6729	150.139	85.97	127
254	21,33	2593	32,40	-0.030340	0.041730	P	21S	69W	1	19.3822	143.981	75.74	124
255	21,33	2593	32,40	-0.029800	0.039920	P	23S	67W	1	23.0738	143.259	78.30	128
256	21,33	2593	32,40	-0.028300	0.041130	P	24S	69W	1	20.0298	145.470	78.15	127
257	21,33	2593	32,40	-0.026330	0.038770	P	28S	67W	1	21.3376	145.818	82.44	138
258	21,33	2593	32,40	-0.027910	0.042370	P	24S	70W	1	19.7097	146.626	77.01	122
259	21,39	2599	38,40	-0.061890	0.041910	P	18N	72W	1	13.3889	124.041	39.90	87

DEPLOY. NUMBER	ROW-COL NUMBERS	GRID SEQ NUMBER	DISPLAY NUMBERS	UX (S/KM)	UY (S/KM)	P-RASE	LAT (DEG)	LONG (DEG)	PRID-RITY	PHASE VELOCITY	BEAN AZIMUTH	RANGE (DEG)	REGJN INDEX
260	21, 6	2630	5, 41	0.114147	0.045545	P	44N	114W	1	8.1368	248.248	6.40	33
261	21, 23	2647	22, 41	0.027330	0.044660	P	22S	139W	1	19.0990	211.465	74.53	631
262	21, 28	2652	27, 41	-0.000780	0.043920	P	40S	105W	1	22.7651	178.982	86.28	692
263	21, 29	2653	28, 41	-0.006090	0.045610	P	37S	97W	1	21.7321	172.395	83.40	686
264	21, 34	2658	33, 41	-0.022240	0.046650	P	15S	73W	1	17.6346	145.351	68.40	117
265	21, 34	2658	33, 41	-0.031950	0.043430	P	10S	70W	1	18.5473	143.659	72.22	118
266	21, 34	2658	33, 41	-0.029640	0.043160	P	21S	71W	1	19.0994	145.521	74.53	122
267	21, 35	2659	34, 41	-0.038320	0.046570	P	8S	72W	1	16.5812	140.551	62.42	113
268	21, 38	2662	37, 41	-0.052770	0.045880	P	9N	72W	1	14.3008	131.005	47.41	100
269	21, 39	2663	38, 41	-0.056790	0.043010	P	12N	71W	1	14.0373	127.138	45.49	97
270	21, 6	2694	5, 42	0.113694	0.047544	P	45N	111W	1	8.1143	247.307	4.00	456
271	21, 15	2703	14, 42	0.064740	0.047909	P	27N	131W	1	12.4164	233.498	27.72	611
272	21, 23	2711	22, 42	0.024640	0.050347	P	19S	132W	1	17.8403	206.077	69.40	632
273	21, 25	2714	25, 42	0.066370	0.048120	P	33S	115W	1	20.6017	187.541	80.08	684
274	21, 26	2714	25, 42	0.055790	0.051440	P	29S	113W	1	19.3181	186.422	75.47	685
275	21, 27	2715	26, 42	0.002120	0.048340	P	34S	109W	1	20.6669	182.511	80.31	684
276	21, 29	2716	27, 42	-0.009900	0.047410	P	35S	105W	1	21.0888	178.912	81.68	692
277	21, 32	2720	31, 42	-0.022310	0.050243	P	21S	92W	1	18.1907	156.056	70.84	683
278	21, 34	2722	33, 42	-0.031860	0.049630	P	12S	76W	1	16.9529	147.285	64.63	115
279	21, 34	2722	33, 42	-0.036240	0.049190	P	8S	75W	1	16.3671	143.620	61.03	112
280	21, 34	2722	33, 42	-0.035290	0.051400	P	6S	77W	1	16.0388	145.527	58.97	111
281	21, 37	2725	36, 42	-0.048310	0.050680	P	7N	75W	1	14.2823	136.371	47.28	99
282	21, 37	2725	36, 42	-0.049780	0.047530	P	7N	73W	1	14.5292	133.675	49.00	99
283	21, 25	2718	25, 43	0.008270	0.054520	P	24S	115W	1	18.1344	188.625	70.62	684
284	21, 34	2786	33, 43	-0.030840	0.054210	P	8S	91W	1	16.0337	150.364	58.94	1.8

DEPLOY. NUMBER	KON-COL NUMBERS	GRID SEC NUMBER	DISPLAY NUMBERS	UX (S/KM)	LY (S/KM)	P-HSF	LAT (DEG)	LONG (DEG)	PRIORITY	PHASE VELOCITY	BEAM AZIMUTH	RANGE (DEG)	GRID INDEX
285	21.34	2786	33,43	-0.031520	0.052100	P	105	79W	1	16.4085	148.856	61.30	109
286	21.34	2786	33,43	-0.033770	0.055290	P	45	81W	1	15.4351	148.564	55.28	110
287	21.35	2787	34,43	-0.037560	0.052520	P	35	77W	1	15.4874	144.429	55.61	110
288	21.36	2788	35,43	-0.039600	0.054590	P	1N	79W	1	14.8279	144.042	51.13	105
289	21.37	2789	36,43	-0.045260	0.052690	P	6N	77W	1	14.3968	139.338	48.07	102
290	21.49	2801	48,43	-0.109499	0.056141	P	44N	100W	1	8.1266	117.145	5.43	462
291	21.29	2845	28,44	-0.007988	0.059007	P	17S	99W	1	16.7941	172.290	63.72	683
292	21.35	2851	34,44	-0.038330	0.058770	P	4N	93W	1	14.2522	146.887	47.06	83
293	21.36	2852	35,44	-0.041730	0.060480	P	9N	84W	1	13.6093	145.395	41.94	78
294	21.36	2852	35,44	-0.042510	0.057790	P	7N	81W	1	13.9390	143.662	44.71	81
295	21.38	2854	37,44	-0.053300	0.056380	P	18N	82W	1	12.8089	136.608	35.12	94
296	21.9	2888	7,45	0.104500	0.061775	P	39N	120W	1	8.2376	239.411	12.37	36
297	21.9	2889	8,45	0.102253	0.063900	P	38N	122W	1	8.4114	237.487	14.86	39
298	21.24	2904	23,45	0.018640	0.063870	P	55	119W	1	15.0298	196.269	52.57	693
299	21.27	2907	26,45	0.007220	0.061250	P	135	112W	1	16.2143	196.723	60.04	694
300	21.27	2907	26,45	0.008040	0.064640	P	95	109W	1	15.4402	183.576	55.31	694
301	21.33	2913	32,45	-0.023630	0.064990	P	0N	91W	1	14.4608	160.019	48.53	697
302	21.35	2916	35,45	-0.039380	0.063800	P	11N	86W	1	13.3378	148.315	39.48	77
303	21.47	2927	46,45	-0.07581	0.061575	P	36N	89W	1	8.6667	122.252	16.39	506
304	21.21	2965	20,46	0.031967	0.069680	P	12N	121W	1	13.0442	204.644	36.77	611
305	21.28	2972	27,46	-0.001390	0.067470	P	55	105W	1	14.8183	178.820	51.06	694
306	21.34	2978	33,46	-0.055440	0.069020	P	14N	91W	1	12.8888	152.821	35.12	70
307	21.35	2979	34,46	-0.041210	0.065560	P	15N	88W	1	12.9139	147.847	35.40	72
308	21.35	2979	34,46	-0.038370	0.065610	P	12N	88W	1	13.1568	149.680	37.81	74
309	21.30	3038	29,47	-0.008990	0.070470	P	2N	101W	1	13.9982	172.770	45.17	693

DEPLOY. NUMBER	RON-COL NUMBERS	GRID SEQ NUMBER	DISPLAY NUMBERS	UX (S/A)	UY (S/A)	PHASE	LAT (DEG)	LONG (DEG)	PRIORITY	PHASE VELOCITY	HEAVY AZIMUTH	RANGE (DEG)	RECEIVE INDEX
310	21.34	3042	33.47	-0.030020	0.072830	P	16N	94W	1	12.6945	157.599	32.72	69
311	21.47	3055	46.47	-0.098385	0.074236	P	30N	94W	1	8.2196	127.663	11.53	482
312	21. 9	3081	8.48	0.096931	0.074199	P	45N	110W	1	8.1106	231.828	3.42	459
313	21.11	3083	10.48	0.086117	0.075083	P	35N	121W	1	8.7526	228.916	16.78	38
314	21.31	3133	30.48	-0.015810	0.078580	P	18N	130W	1	12.6759	168.624	29.65	59
315	21.31	3133	30.48	-0.018230	0.077690	P	17N	99W	1	12.5313	166.794	30.38	58
316	21.32	3134	31.48	-0.020890	0.076610	P	16N	98W	1	12.5933	164.747	31.24	58
317	21.32	3134	31.48	-0.024110	0.075180	P	15N	96W	1	12.6660	162.219	32.31	66
318	21.13	3166	9.49	0.091995	0.079242	P	38N	118W	1	8.2363	229.259	12.29	40
319	21.26	3162	25.49	0.008110	0.080500	P	20N	109W	1	12.3598	185.753	27.18	53
320	21.45	3181	44.49	-0.090696	0.082681	P	42N	99W	1	8.1482	132.353	7.32	463
321	21.12	3212	11.50	0.079330	0.084525	P	34N	119W	1	8.6266	223.184	16.19	43
322	21.11	3275	10.51	0.086083	0.088019	P	43N	111W	1	8.1224	224.363	5.00	460
323	21.12	3276	11.51	0.080581	0.091818	P	39N	114W	1	8.1857	221.271	9.74	37
324	21.12	3276	11.51	0.081176	0.090274	P	37N	115W	1	8.2369	221.962	12.32	41
325	21.13	3277	12.51	0.077580	0.088500	P	34N	118W	1	8.4937	221.219	15.44	43
326	21.41	3305	40.51	-0.067400	0.089656	P	32N	94W	1	8.9154	143.065	17.42	504
327	21.13	3341	12.52	0.075842	0.096703	P	41N	112W	1	8.1369	218.136	6.45	478
328	21.25	3353	24.52	0.013000	0.094040	P	25N	109W	1	13.5314	187.869	21.55	49
329	21.15	3437	14.53	0.069734	0.099946	P	37N	114W	1	8.2056	214.934	10.85	41
330	21.16	3438	15.53	0.062394	0.099465	P	33N	115W	1	8.5168	212.100	15.58	45
331	21.17	3409	16.53	0.058639	0.096841	P	32N	116W	1	9.8331	211.195	17.11	48
332	21.23	3476	19.54	0.039270	0.102610	P	30N	114W	1	9.1253	210.433	18.33	49
333	21.43	3496	39.54	-0.063571	0.105077	P	44N	104W	1	8.1687	148.970	3.13	460
334	21.17	3537	16.55	0.058667	0.107487	P	39N	112W	1	8.1662	218.626	8.64	470

DEPLOY. NUMBER	ROW-COL NUMBERS	GRID SEQ NUMBER	DISPLAY NUMBERS	UX (S/KM)	UY (S/KM)	PHASE	LAT (DEG)	LONG (DEG)	PRIORITY	PHASE VELOCITY	BEAM AZIMUTH	RANGE (DEG)	REGID INDEX
335	21,19	3603	18,56	0.046416	0.113755	P	40N	110W	1	8.1393	252.197	6.65	478
336	21,20	3620	35,56	-0.045552	0.112963	P	36N	101W	1	8.2163	158.021	11.38	499
337	21,21	3668	19,57	0.040126	0.216639	P	44N	107W	1	8.1071	198.984	2.80	460
338	21,22	3677	28,57	-0.004529	0.115885	P	31N	105W	1	8.6227	177.762	16.17	518
339	21,26	3738	25,58	0.007541	0.121820	P	37N	107W	1	8.1932	183.542	10.19	496
340	21,29	3741	28,58	-0.006248	0.123156	P	43N	106W	1	8.1094	177.096	3.20	460
341	21,31	3743	30,58	-0.017137	0.121640	P	40N	105W	1	8.1406	171.981	6.75	479